Photoswitchable Tetraethynylethene-Dihydroazulene Chromophores

by **Luca Gobbi**, **Paul Seiler**, and **François Diederich***

Laboratorium für Organische Chemie, ETH-Zentrum, Universitätstrasse 16, CH-8092 Zürich

Volker Gramlich

Laboratorium für Kristallographie, ETH-Zentrum, Sonneggstrasse 5, CH-8092 Zürich

and **Corinne Boudon**, **Jean-Paul Gisselbrecht**, and **Maurice Gross**

Laboratoire d'Electrochimie et de Chimie Physique du Corps Solide, Université Louis Pasteur, C.N.R.S.: U.M.R. No. 7512, Faculté de Chimie, 4 rue Blaise Pascal, F-67000 Strasbourg

The synthesis, characterization, and photophysical as well as electrochemical properties of the photochromic hybrid systems **11**–**16** and **18**, which contain photoswitchable tetraethynylethene (TEE; 3,4-diethynylhex-3-ene-1,5-diyne) and dihydroazulene (DHA) moieties, are presented. The molecular photoswitches were synthesized by a *Sonogashira* cross-coupling reaction between an appropriate TEE precursor (**6**–**10** and **17**) and an iodinated DHA **1** or its vinylheptafulvene (VHF) isomer (**4**) (*Schemes 5–7*). X-Ray crystal structures of five DHA derivatives (**1**, *trans*-**11a**, *cis*-**11a**, **12**, and **13**) are discussed (*Figs. 2–5*). In all compounds, the cyclohexatriene moiety of the DHA chromophore adopts a clear boat conformation (*Table 1*). Presumably due to crystal-packing effects, the arylated TEE moieties in the hybrid systems show substantial distortions from planarity, with the dihedral angles between the planes of the central TEE core and the adjacent aryl substituents amounting to 44°. The switching properties were investigated by electronic absorption spectroscopy. Upon light absorption, DHAs **1**, **12**–**16**, and **18** underwent retro-electrocyclization in solution to give the corresponding VHFs (*Figs. 6*, *11*, and *12*). The reaction is thermally reversible, with half-lives $\tau_{1/2}$ between 3.9 and 5.8 h at 25° in CH_2Cl_2 (*Figs. 7* and *13* and *Table 3*). A comparatively slower (*E*) → (*Z*) isomerization process about the central C=C bond of the TEE moiety was also observed. The *N*,*N*-dimethylanilino-(DMA) substituted TEE-DHA hybrid systems *trans*-**11a** and *cis*-**11a** did not react to the corresponding VHFs upon irradiation (*Scheme 9*). Instead, only the reversible (*E*) → (*Z*) photoisomerization of the TEE core occurred (*Fig. 16* and *Table 4*). This process was further investigated for photofatigue by electronic-emission spectroscopy (*Fig. 17*). After protonation of the DMA group, the usual DHA → VHF photoreaction took place. Compound **11** represents a three-way chromophoric molecular switch with three addressable sub-units (TEE core, DHA/VHF moiety, and proton sensitive DMA group) that can undergo individual, reversible switching cycles (*Scheme 9*). A process modeling the function of an 'AND' logic gate (*Fig. 19*) and three write/erase processes could be performed with this system. Cyclic and linear sweep-voltammetry studies in CH_2Cl_2 (+ Bu_4NPF_6) revealed the occurrence of characteristic first-reduction steps in the TEE-DHA hybrid systems between −1.6 and −1.8 V *vs.* Fc/Fc^+ (ferrocene/ferricinium couple) (*Table 5*). Oxidations occur at *ca.* +1.10 V. After photoisomerization to the VHF derivatives, reduction steps at more positive and oxidation steps at more negative potentials were recorded. No DHA → VHF isomerization took place upon electrochemical oxidation or reduction (*Fig. 20*).

1. Introduction. – Molecular switches are systems that possess at least two reversibly interconvertible states [1]. Their study has attracted increasing interest in recent years, owing to their potential as functional building blocks for molecular devices [2]. Possible applications range from molecular-scale information processing and reversible high-density data storage [3], to biomimetic engineering [4]. Photoresponsive systems [5] have attracted particular attention, since the use of light as an external switching

stimulus allows for fast and clean processes (for recent reviews, see [6]). Some of the most promising and most widely used systems reported to date are *i*) the (*Z*)-1,2-di(3-thienyl)ethenes developed by *Irie* and co-workers [7] and successfully used by other research groups [8], *ii*) the ethene-based chiroptical photoswitches studied by *Feringa* and co-workers [9], *iii*) spiropyranes [10], *iv*) fulgides [11], and *v*) azobenzenes [12]. In 1984, *Daub et al.* first reported the photochromic properties of dihydroazulenes (DHA; *Scheme 1*) [13]. DHAs react after light irradiation in a 10-electron *retro*-electrocyclization to vinylheptafulvenes (VHF), that, in turn, undergo a thermal cyclization back to the starting materials [14].

Scheme 1. *The Dihydroazulene (DHA)-Vinylheptafulvene (VHA) Molecular Photoswitch* [13][14]

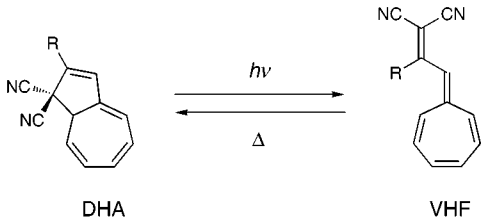

With aryl-substituted tetraethynylethene (TEE; 3,4-diethynylhex-3-ene-1,5-diyne) derivatives [15], we recently introduced a new class of molecular photoswitches that undergo two-way photochemical interconversions, not perturbed by thermal isomerization pathways [16]. Here, we describe the synthesis of a new series of photochromic hybrid systems containing both TEE and DHA moieties as individually addressable, photoswitchable subunits (*Fig. 1*). The structural and electronic characteristics of these novel chromophores are reported, as well as detailed investigations exploring how the switching capacity of one sub-unit is affected by the presence of the second one in the same molecule (for a preliminary communication of parts of this work, see [17]).

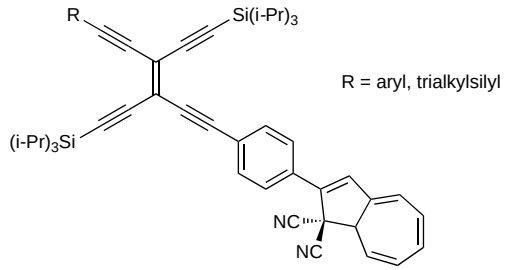

Fig. 1. *Hybrid systems containing tetraethynylethene (TEE) and dihydroazulene (DHA) moieties as individually addressable photoswitchable subunits*

2. Results and Discussion. – 2.1. *Synthesis.* Two routes for the synthesis of DHAs have been reported by *Daub* and co-workers [13][18–20]. The first one involves a [8 + 2] cycloaddition between 8-methoxyheptafulvene and a 1,1-dicyanoethylene (= but-2-enedinitrile) derivative, followed by elimination of MeOH to produce directly the thermally stable dihydroazulene (DHA) chromophore [19]. An alternative protocol starts from a tropylium salt and acetophenone derivatives, and provides first the

vinylheptafulvene (VHF) chromophore, which subsequently undergoes thermal isomerization to the DHA form [20]. The latter route was initially used to prepare DHA **1** bearing a 4-iodophenyl substituent for attachment to tetraethynylethene (TEE) derivatives with a free ethynyl group by Pd^0-catalyzed *Sonogashira* cross-coupling [21] (*Scheme 2*). Commercially available 4-iodoacetophenone underwent an acid-catalyzed nucleophilic addition to tropylium tetrafluoroborate to provide ketone **2**, which produced the dicyanoethene **3** by acid-catalyzed *Knoevenagel* condensation with malononitrile. Hydride abstraction with tritylium tetrafluoroborate to form the tropylium cation and subsequent deprotonation afforded VHF **4** as a mixture with DHA isomer **1**. Upon heating this mixture to 80° in the dark, the isomeric equilibrium was completely shifted to the thermally stable DHA form, which was isolated in 70% yield (starting from **3**). Analytically pure **4** was obtained in high yield (91%) as deep-red crystals by irradiating a saturated solution of **1** in hexane at 366 nm.

Scheme 2. *Synthesis of the 4-Iodophenyl-Substituted DHA* **1** *and VHF* **4**

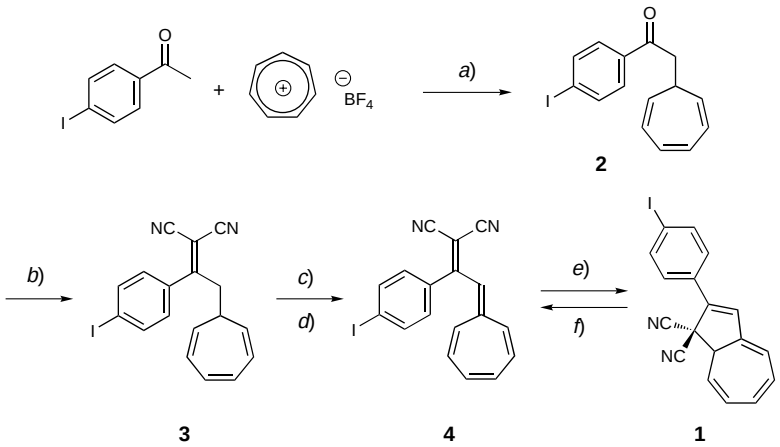

a) AcOH, MeOH, 20°, 6 h; 50%. *b*) Malononitrile, AcOH, NH_4OAc, PhMe ↑↓, 8 h; 75%. *c*) Ph_3CBF_4, $ClCH_2CH_2Cl$, 80°, 1 h. *d*) Et_3N, PhMe, 0° → 20°, 1 h. *e*) 80°, in the dark, 1 h; 70% (from **3**). *f*) Hexane, hν (366 nm), 20°, 6 h; 91%.

All attempts to produce multigram quantities of **1** by the protocol described in *Scheme 2*, however, failed. On the larger scale, the *Knoevenagel* condensation of **2** with malononitrile worked only poorly or even not at all. At prolonged reaction times, cleavage of the cycloheptatriene group was observed, leading to dicarbonitrile **5** in 69% yield (*Scheme 3*). We assume that, in a first step, the tropylium cation is eliminated in the reversal of the addition reaction that produced **2** (*Scheme 2*), and that the 4-iodoacetophenone formed subsequently undergoes the *Knoevenagel* condensation under formation of **5**.

Taking these observations into account, we modified the large-scale synthesis of **4** by performing in the first step the *Knoevenagel* condensation between 4-iodoacetophenone and malononitrile (*Scheme 4*). When the reaction was conducted in benzene in the presence of AcOH and NH_4OAc, dinitrile **5** was obtained in 89% yield. The use of toluene as the solvent was less satisfactory, and almost no conversion was observed in

Scheme 3. *Major Side Reaction in the Large-Scale* Knoevenagel *Condensation of* **2** *with Malononitrile*

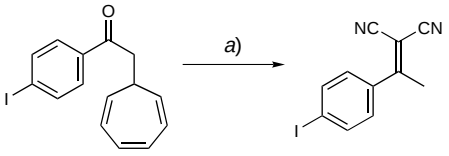

2 **5**

a) Malononitrile, AcOH, NH_4OAc, PhMe, ↑↓, 4 d; 69%.

EtOH with piperidine as the catalyst. Since the acid-catalyzed nucleophilic addition of 4-iodoacetophenone to the tropylium cation had only provided a moderate yield (50%) of **2** (*Scheme 2*), we decided to explore the corresponding nucleophilic addition of **5** under basic conditions. First attempts to deprotonate **5** with DBU (1,8-diazabicyclo[5.4.0]undec-7-ene) in toluene at 40° or −10° in the presence of tropylium tetrafluoroborate failed, leading only to decomposition products. At −78° in the presence of 1.1 equiv. of DBU, the desired reaction took place and afforded a mixture **5**/**3** in a 1.3 : 1 ratio. A larger excess of DBU led to the formation of major, non-identified side products, possibly initiated by deprotonation of **3**. Gratifyingly, changing to the milder base Et_3N in CH_2Cl_2 at −78° provided the desired product in quantitative yield. The subsequent dehydration of **3** to **4** (and the thermal conversion to **1**) on the multigram scale worked as described above (*Scheme 2*). This new synthetic route not only provided sufficient quantities of **1** for the projects described in this manuscript but also allowed the preparation of a highly efficient polymeric waveguide doped with this molecular switch [22].

Scheme 4. *Alternative Synthesis of Dinitrile* **3**, *the Precursor to the Molecular Switch* **1**

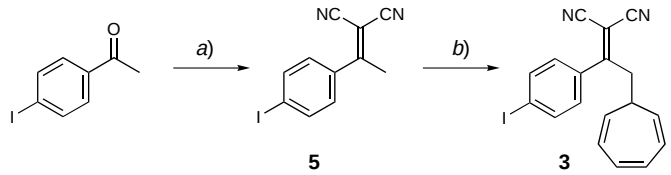

5 **3**

a) Malononitrile, AcOH, NH_4OAc, PhH, ↑↓, 3 d; 89%. *b*) Et_3N, tropylium tetrafluoroborate, CH_2Cl_2, −78°, 1 h; 100%.

A series of TEE derivatives, with different substituents in the *trans*-position to the ethynyl residue ultimately bearing the DHA/VHF moiety, was prepared by previously introduced routes [15c]. Mono-deprotected TEE **6** [15c] was cross-coupled to various aryl iodides (4-R-C_6H_4I; R = Me_2N, NO_2, MeO, H) under *Sonogashira* conditions [21][23], thereby affording the arylated TEEs **7** [15c], **8** [15c], **9**, and **10** (*Scheme 5*). The anisole derivative **9** turned out to be very sensitive towards light and readily underwent rapid *trans* → *cis* isomerization of the TEE moiety. A slower *trans* → *cis* isomerization was also observed for **7** and **8** upon irradiation at 366 nm or prolonged exposure to sunlight. The Me_3Si group was removed with K_2CO_3 in MeOH/THF, and the mono-deprotected arylated TEEs were coupled to the iodinated VHF derivative **4**,

yielding the *trans*-configured TEE-DHA hybrid compounds *trans*-**11a** and **12**–**14** as thermally stable materials (after VHF → DHA isomerization). Similarly, cross-coupling between **6** and **4** gave the hybrid derivative **15**. To prevent photochemical *trans* → *cis* isomerizations, reactions were usually performed in the dark. The VHF derivative **4** was preferentially used (instead of isomeric **1**) to form the hybrid compounds, since it was obtained in particularly high purity by recrystallization, which, in return, benefited the yield of the cross-coupling reaction.

Scheme 5. *Synthesis of the TEE-DHA Hybrid Derivatives* trans-**11a** *and* **12**–**15**

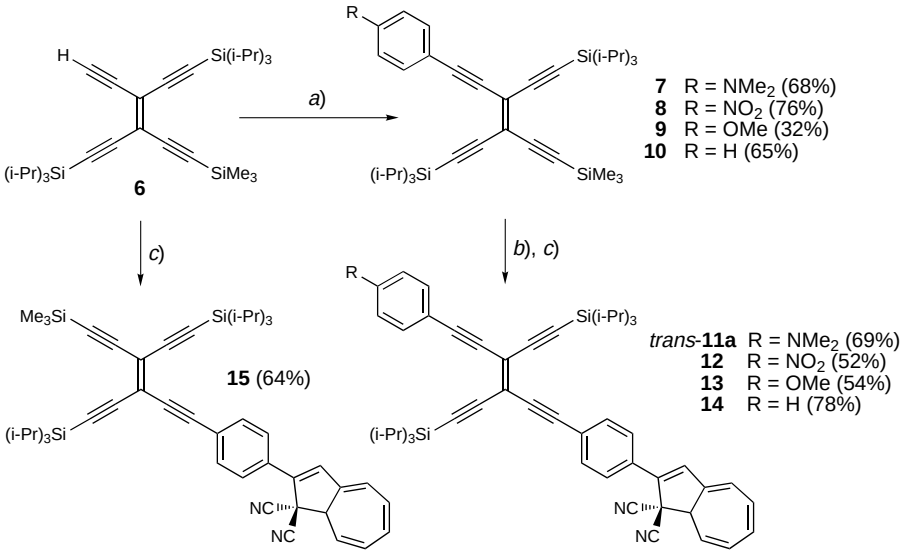

a) $[PdCl_2(PPh_3)_2]$, CuI, Bu_4NBr, $(i\text{-}Pr)_2NH$, THF, 4-Me_2N-C_6H_4I (→ **7**), 4-O_2N-C_6H_4I (→ **8**), 4-MeO-C_6H_4I (→ **9**), PhI (→ **10**), 20°, 45 min – 15 h. *b*) K_2CO_3, MeOH, THF, 20°, 60–90 min. *c*) **4**, $[PdCl_2(PPh_3)_2]$, CuI, Bu_4NBr, $(i\text{-}Pr)_2NH$, THF, 20°, 1–17 h. All steps were usually performed in the dark to prevent *trans* → *cis* isomerization.

However, DHA isomer **1** could also be used in the *Sonogashira* cross-coupling reaction, as illustrated by the preparations of thiophene derivative **16** (obtained by the sequence **6** → **17** → **16**; *Scheme 6*) and TEE-DHA hybrid **18** bearing three $(i\text{-}Pr)_3Si$ groups (obtained by the sequence **19** [24] → **20** → **18**; *Scheme 7*). The reaction of **19** with 3.3 equiv. of $(i\text{-}Pr)_2NLi$ (LDA) in THF at −78° gave a green monometallated lithium acetylide that was silylated with $(i\text{-}Pr)_3SiOSO_2CF_3$ to give **20** in good yield (88%). While the silylation with $(i\text{-}Pr)_3SiOSO_2CF_3$ was complete after a few minutes at −78°, the analogous reaction with $(i\text{-}Pr)_3SiCl$ took several hours and gave only poor yields.

For investigations of the *trans*/*cis* photoisomerization between *trans*-**11a** and *cis*-**11a**, a sample of *cis*-**11a** was prepared by irradiating *trans*-**11a** in CH_2Cl_2 at 366 nm and separating the resulting isomeric mixture by column chromatography (*Scheme 8*).

2.2. *X-Ray Crystal-Structure Analyses.* X-Ray crystal structures of five DHA derivatives were solved. Yellow crystals of **1** were grown at room temperature from

Scheme 6. *Synthesis of the TEE-DHA Hybrid Derivative* **16** *Starting from* **1**

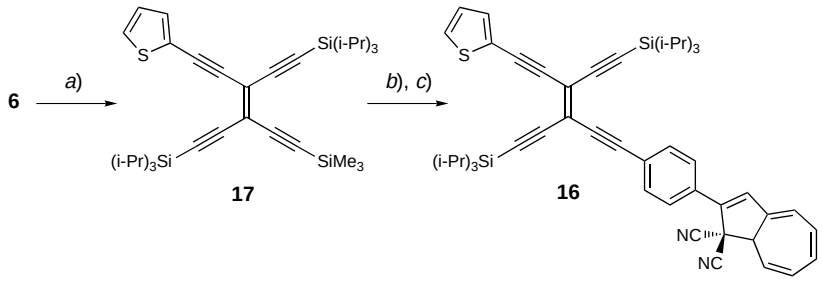

a) [$PdCl_2(PPh_3)_2$], CuI, 2-iodothiophene, $(i\text{-}Pr)_2NH$, THF, 20°, 20 min; 64%. *b*) K_2CO_3, MeOH, THF, 20°, 3 h. *c*) [$Pd(PPh_3)_4$], CuI, **1**, $(i\text{-}Pr)_2NH$, THF, 20°, 18 h; 45% (steps *b* and *c*).

Scheme 7. *Synthesis of TEE-DHA Hybrid Derivative* **18**

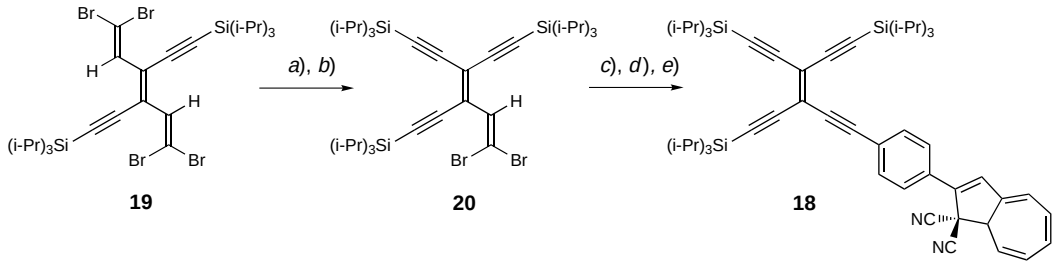

a) LDA (3.3 equiv.), THF, −78°, 15 min. *b*) $(i\text{-}Pr)_3SiOSO_2CF_3$, THF, −78°, *ca.* 5 min, then −78° → 0°; 88% (steps *a* and *b*). *c*) LDA, THF, −78°, 15 min. *d*) Sat. aq. NH_4Cl soln. *e*) [$PdCl_2(PPh_3)_2$], CuI, **1**, $(i\text{-}Pr)_2NH$, THF, 20°, 11 h; 74% (steps *c*, *d*, and *e*).

Scheme 8. *Synthesis of* cis-**11a**

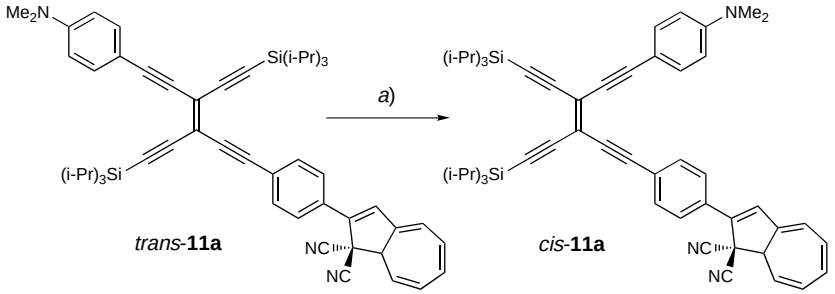

a) *hv* (366 nm), CH_2Cl_2, 20°, 3.5 h; 39%.

Et_2O/hexane. The racemic compound, with a stereogenic center at C(9), crystallizes in the $P\bar{1}$ space group, with the elemental cell occupied by two molecules. Its structure (*Fig. 2, a*) closely resembles those previously reported for DHA derivatives by *Daub* and co-workers [18a][25], with the seven-membered ring adopting a boat conformation ($\alpha = 54.3°$ and $\beta = 28.0°$; *Fig. 2, b*). A clear bond-length alteration is apparent in the linearly π-conjugated octatetraene chromophore of the DHA moiety, with C–C bond lengths of 1.440(7) – 1.431(7) Å and C=C bond lengths of 1.327(7) – 1.353(6) Å.

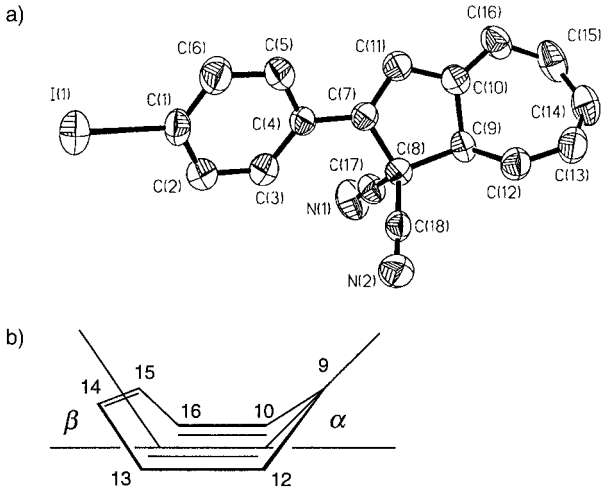

Fig. 2. a) *ORTEP Plot of* **1**. Arbitrary numbering. Atomic-displacement parameters obtained at 293 K are drawn at the 50% probability level. b) *Definition of the angles α and β describing the boat conformation of the cycloheptatriene ring in DHA derivatives* [19]. Selected bond lengths [Å] and bond angles [°]: C(4)–C(7) 1.463(6), C(7)–C(11) 1.342(6), C(10)–C(11) 1.429(6), C(10)–C(16) 1.353(6), C(15)–C(16) 1.431(7), C(14)–C(15) 1.327(7), C(13)–C(14) 1.440(7), C(12)–C(13) 1.342(7), C(9)–C(12) 1.505(6), C(9)–C(10) 1.514(6), C(8)–C(9) 1.564(6); C(8)–C(7)–C(11) 108.8(4), C(7)–C(11)–C(10) 113.4(4), C(11)–C(10)–C(16) 130.0(4), C(10)–C(16)–C(15) 123.8(5), C(16)–C(15)–C(14) 126.6(4), C(15)–C(14)–C(13) 125.4(5), C(14)–C(13)–C(12) 125.7(5), C(13)–C(12)–C(9) 119.9(4), C(12)–C(9)–C(10) 107.1(3), C(9)–C(10)–C(16) 121.6(4), C(9)–C(10)–C(11) 108.4(4), C(8)–C(9)–C(10) 103.3(3), C(7)–C(8)–C(9) 104.1(3), C(17)–C(8)–C(18) 107.2(3). These bond lengths and angles are also characteristic for the DHA moieties in the solid-state structures of the TEE-DHA hybrid materials.

This boat conformation is also observed for the DHA chromophores in the X-ray crystal structures of the TEE hybrid systems (*Table 1* and *Figs. 3–5*). Appropriate single crystals of *cis*-**11a**, **12**, and **13** were grown by slow evaporation of CH_2Cl_2/MeCN solutions, whereas those of *trans*-**11a** were obtained from MeOH (for a view on the X-ray crystal structure of *trans*-**11a**, see [17]). Compounds *trans*-**11a** and **13** crystallize in the centrosymmetric $P\bar{1}$ space group (two molecules in the unit cell), whereas **12** crystallizes in *P*1 (one molecule per unit cell) and *cis*-**11a** in the *P*2(1)/*c* space group (six molecules per unit cell). As reported for other trialkylsilyl-protected TEEs, some disorder occurs in the $(i\text{-}Pr)_3Si$ groups, which has a negative impact on the structural accuracy [15c]. Bond angles and bond lengths in the arylated TEE cores were in the range observed in similar X-ray crystal structures [15][16b][26]. A nearly perfect coplanarity between the TEE core and the adjacent aryl rings was observed only for

Table 1. *Angles α and β Defining the Boat Conformation of the Cycloheptatriene Ring in DHA Derivatives and Dihedral Angles between the Central TEE Core and the Adjacent Aryl Substituents A and B*

Compound	α [°]	β [°]	A/TEE [°]	B/TEE [°]
1	54	28	–	–
trans-**11a** [a])	[b])	[b])	17	~0.1
cis-**11a**	46	24	44	30
12	47	22	6	26
13	47	24	21	22

[a]) From [17]. [b]) Not determined due to static disorder in the cycloheptatriene ring.

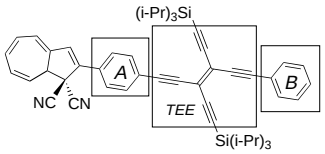

trans-**11a** [17]; in all other structures, the aryl rings show significant deviations from the TEE plane (*Table 1*), probably due to packing effects.

This distortion is particularly strong for *cis*-**11a**, in which the dihedral angles between the TEE core and the two adjacent aryl substituents amount to 30 and 44°, respectively. The five-membered ring in the DHA moiety is nearly coplanar with the adjacent phenylene ring, which is twisted by *ca.* 44° out of the plane of the central TEE core. Such geometry is undoubtedly imposed by the observed self-assembly of solid *cis*-**11a** into supramolecular dimers (*Fig. 3, b*). In these dimers formed in the crystal lattice, two neighboring *cis*-**11a** molecules arrange in such a way as to form several close intermolecular contacts between their DHA-C_6H_4-TEE-DMA moieties (DMA = *N*,*N*-dimethylaniline), whereas the (i-Pr)$_3$Si groups point away from the dimeric assembly to interact with the same groups of neighboring dimers. The arylated DHA moieties adopt an antiparallel arrangement in the dimer, with the aryl rings positioned above the cycloheptatriene rings (shortest contact C(4)$\cdots$C(20) = 3.45 Å). The latter, in return, interact *via* their C(21)–C(23) bonds with the neighboring DMA rings (shortest contact C(22)$\cdots$C(31) = 3.53 Å).

2.3. *Photophysical Properties.* A solution of yellow DHA **1** displays photochromic properties when exposed to sunlight. The underlying process is accelerated when UV light of 366 nm is used. The isosbestic points in the UV/VIS spectra are in accordance with two species equilibrating. In a first study, the light-induced ring-opening of **1** to **4** was investigated in CH_2Cl_2 (*Fig. 6*). A *sterilAir BLB-8* lamp, commonly employed to view TLC plates with fluorescent coatings, was used as light source. After irradiation (366 nm) for *ca.* 20 s, a complete conversion of **1** to **4** was observed under these conditions. The isomerization was followed by UV/VIS spectroscopy, monitoring the decrease in intensity of the characteristic absorption band of **1** at λ_{max} of 365 nm and the concomitant increase of a new band for **4** at λ_{max} of 478 nm. The thermal back reaction from **4** to **1** was investigated in CH_2Cl_2 at 27° (*Fig. 7*). The half-life $t_{1/2}$ of **4** under these conditions is 5.8 h. In the crystal, **4** is stable; its deep-red color prevails until the melting point is reached at 116°, when an instantaneous color loss is observed. For this reason, a

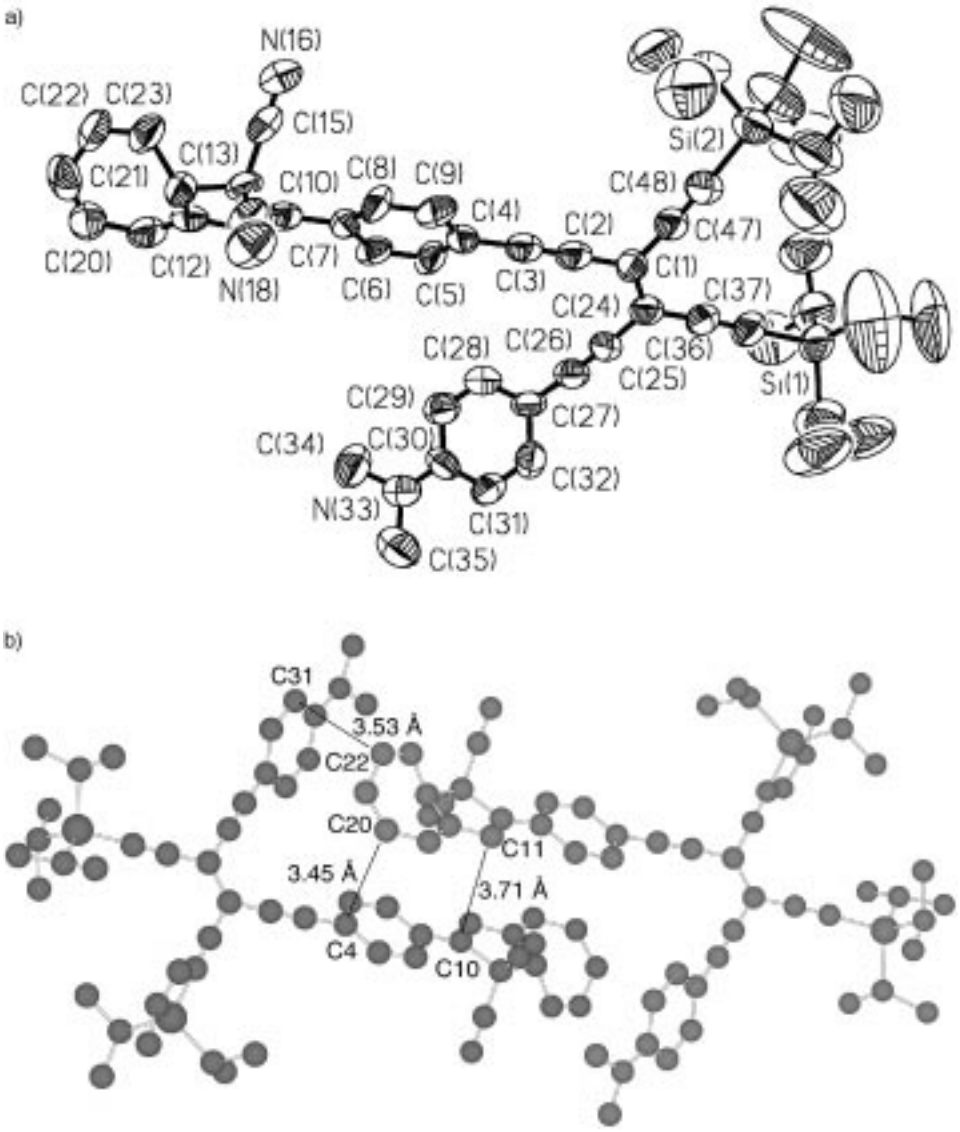

Fig. 3. a) *ORTEP Plot of* cis-**11a**. Arbitrary numbering. Atomic-displacement parameters obtained at 293 K are shown at the 50% probability level. b) *Aryl-DHA interactions in the supramolecular dimer formed by* cis-**11a** *in the crystal.* Bond lengths [Å] and angles [°] in the TEE core: C(2)–C(3) 1.200(13), C(1)–C(2) 1.429(12), C(1)–C(47) 1.442(12), C(47)–C(48) 1.196(11), C(1)–C(24) 1.373(10), C(24)–C(25) 1.423(12), C(25)–C(26) 1.180(13), C(24)–C(36) 1.416(12), C(36)–C(37) 1.195(11); C(1)–C(2)–C(3) 177.7(9), C(2)–C(1)–C(47) 115.8(9), C(1)–C(47)–C(48) 177.3(9), C(2)–C(1)–C(24) 121.3(9), C(47)–C(1)–C(24) 122.9(8), C(1)–C(24)–C(25) 119.6(9), C(24)–C(25)–C(26) 176.6(8), C(25)–C(24)–C(36) 119.8(9), C(1)–C(24)–C(36) 120.6(8), C(24)–C(36)–C(37) 176.8(9).

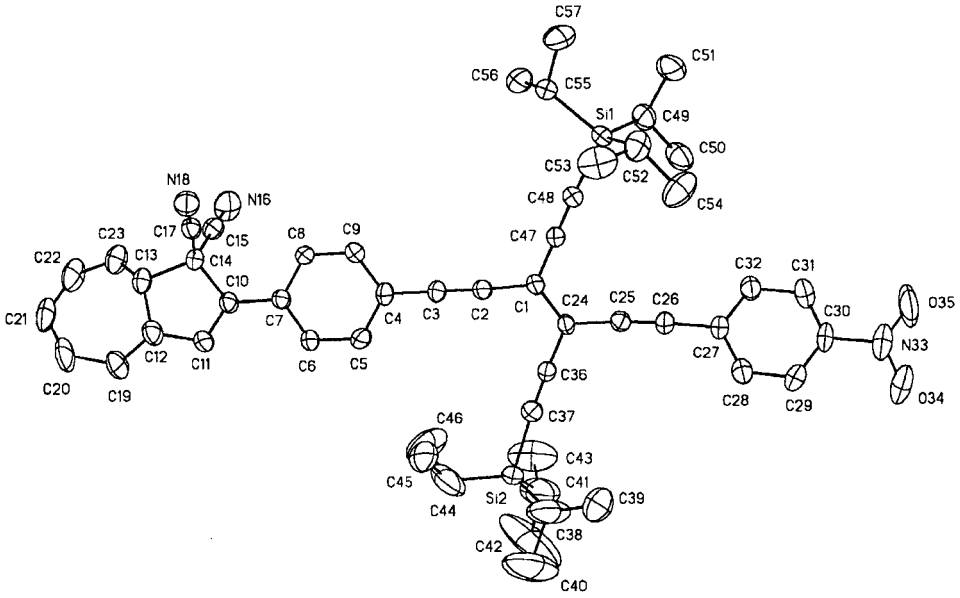

Fig. 4. *ORTEP Plot of* **12**. Arbitrary numbering. Atomic-displacement parameters obtained at 295 K are shown at the 30% probability level. Bond lengths [Å] and angles [°] in the TEE core: C(2)–C(3) 1.207(8), C(1)–C(2) 1.409(8), C(1)–C(47) 1.434(8), C(47)–C(48) 1.207(8), C(1)–C(24) 1.367(8), C(24)–C(25) 1.445(8), C(25)–C(26) 1.196(9), C(24)–C(36) 1.421(8), C(36)–C(37) 1.195(9); C(1)–C(2)–C(3) 175.8(6), C(2)–C(1)–C(47) 118.3(5), C(1)–C(47)–C(48) 177.7(6), C(2)–C(1)–C(24) 120.1(5), C(47)–C(1)–C(24) 121.5(5), C(1)–C(24)–C(25) 122.0(5), C(24)–C(25)–C(26) 174.0(7), C(25)–C(24)–C(36) 115.6(5), C(1)–C(24)–C(36) 122.4(5), C(24)–C(36)–C(37) 177.5(7).

nonreactive s-*trans*-VHF conformation (*Fig. 8*) is postulated for **4** in the solid state [18a].

All investigated DHA-TEE hybrid derivatives (*trans*-**11a**, *cis*-**11a**, **12**–**16**, and **18**) were stable crystalline yellow-to-orange-colored solids with high melting points between 151° and 222°. These compounds are not photochromic in the crystal. After irradiation in solution, a dark-orange coloration was observed for all with the exception of *trans*-**11a** and *cis*-**11a**. *Fig. 9* shows the electronic-absorption spectra of all DHA derivatives synthesized in this work. Compared to **1**, the TEE-DHA hybrid derivatives show a strong enhancement of the molar extinction coefficient and a large bathochromic shift of the longest-wavelength absorption band. Correspondingly, the optical end-absorption shifts to lower energy. The two tris-trialkylsilylated compounds **15** and **18** expectedly display nearly identical UV/VIS spectra. They both feature a shoulder around 360 nm, which is related to a local electronic transition in the DHA moiety. The extension of the π-system by addition of a second aryl substituent to the TEE core (**12**–**14** and **16**) leads to a further increase in the molar extinction coefficient of the longest-wavelength absorption maximum, which, together to the optical end-absorption, appears at even lower energy. All these data are in agreement with extended π-electron delocalization over the entire conjugated π-chromophore in these molecules.

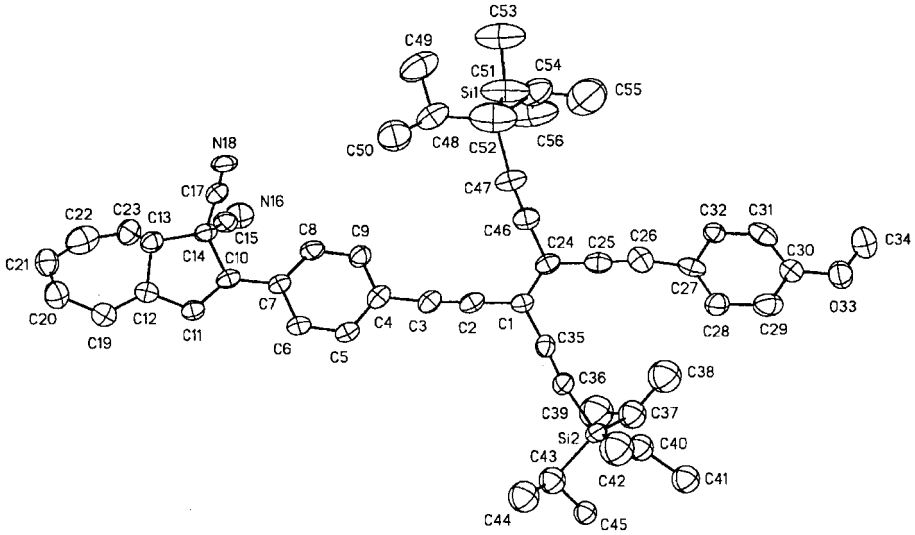

Fig. 5. *ORTEP Plot of* **13**. Arbitrary numbering. Atomic-displacement parameters obtained at 213 K are shown at the 30% probability level. Bond lengths [Å] and angles [°] in the TEE core: C(2)–C(3) 1.195(11), C(1)–C(2) 1.428(12), C(1)–C(35) 1.424(11), C(35)–C(36) 1.216(11), C(1)–C(24) 1.351(11), C(24)–C(25) 1.448(13), C(25)–C(26) 1.212(13), C(24)–C(46) 1.452(12), C(46)–C(47) 1.200(11); C(1)–C(2)–C(3) 179.5(8), C(2)–C(1)–C(24) 121.6(7), C(1)–C(24)–C(25) 123.5(7), C(24)–C(25)–C(26) 176.9(9), C(1)–C(24)–C(46) 122.5(8), C(24)–C(46)–C(47) 176.6(10), C(46)–C(24)–C(25) 114.0(8), C(2)–C(1)–C(35) 118.4(7), C(24)–C(1)–C(35) 120.0(7), C(1)–C(35)–C(36) 177.7(8).

Efficient intramolecular donor-acceptor interactions [15c] are at the origin of the strong bathochromic shifts measured for the longest-wavelength absorption maximum and the optical end-absorption of the DMA derivatives *trans*-**11a** and *cis*-**11a**. The red-shifted position of their longest-wavelength absorption band ($\lambda_{max} = 464$ nm) – with high intermolecular charge-transfer character – clearly indicates a strong conjugative interaction between the DHA acceptor and the DMA donor. This interaction is much stronger than the one between this acceptor and the 2-thienyl donor ($\lambda_{max} = 420$ nm) in **16** or the 4-methoxyphenyl donor ($\lambda_{max} = 419$ nm) in **13** (*Table 2*), which both lack such a red-shifted band. After protonation of the DMA group in *trans*-**11a** or *cis*-**11a** with CF_3CO_2H, the charge-transfer absorption vanishes, and their spectra resemble those of the other TEE-DHA conjugates (*Fig. 9* and *Table 2*). In further support of the proposed intermolecular charge-transfer interaction, the longest-wavelength absorption maximum of *trans*-**11a** is shifted hypsochromically when the solvent is changed from CH_2Cl_2 to hexane ($\lambda_{max} = 443$ nm), an environment with a very limited capacity for stabilizing polar states (*Fig. 10*).

The photochromism of the TEE-DHA hybrid derivatives **12**–**16** and **18** (for the special behavior of *trans*-**11** and *cis*-**11**, see *Sect. 2.4* below) was investigated in CH_2Cl_2 solutions. The orange color that appears after irradiation derives from a new band in the UV/VIS spectra with a maximum at *ca.* 480 nm. By comparison with the spectrum of **4** (*Figs. 6* and *7*), this band is assigned to the isomeric VHF form. Parallel to the appearance of this band, the intensity of the characteristic DHA absorption around

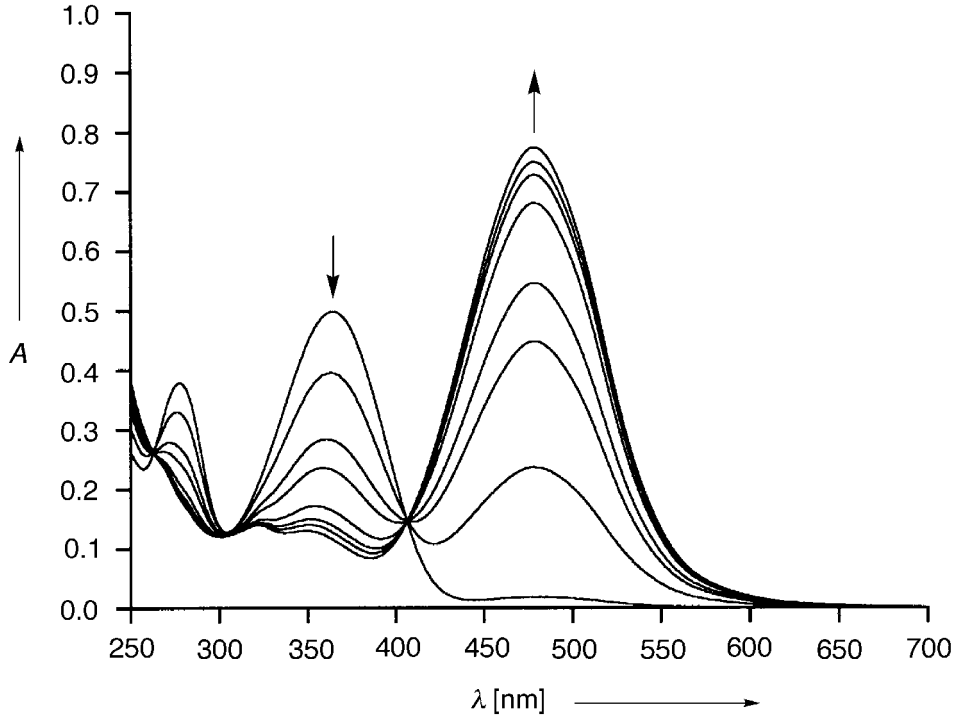

Fig. 6. *UV/VIS Spectra recorded during irradiation of* **1** *at* $\lambda = 366$ *nm in* CH_2Cl_2 ($c = 2.33 \cdot 10^{-5}$ M). Spectra recorded after 0, 2, 4, 6, 8, 10, 12, and 32 s.

404 – 420 nm decreases, which is a clear indication that a photochemical switching process is operative. This process is illustrated in *Fig. 11*, which depicts the UV/VIS spectra recorded during the irradiation (366 nm, 7 min) of **14** in CH_2Cl_2. Since the TEE moiety is also photoactive [16] (as mentioned in the *Introduction*), the DHA/VHF isomerization could potentially also be accompanied by a *trans*/*cis* isomerization around its central C=C bond. However, the occurrence of clean isosbestic points shows that only two species are at equilibrium and that the *trans*/*cis* isomerization process is much slower than the DHA → VHF *retro*-electrocyclization. The photoreaction of the TEE group can, indeed, be observed, when samples are left for prolonged time in the light. To prove that the changes in the absorption spectra arise from the DHA → VHF isomerization process, compound **18** was studied with monochromatic light (405 nm) from a fluorimeter light source (*Fig. 12*). Because of three $(i\text{-}Pr)_3Si$ substituents at the TEE core, the *trans/cis* isomerization is a degenerate process and leads to identical compounds. Therefore, light-induced structural changes involve only isomerization of the DHA moiety, leading to VHF derivative **21**.

A closer look at the UV/VIS spectra revealed that the characteristic absorption bands of the starting TEE-DHA hybrid compounds around 404 – 420 nm never fully faded away. An isomerization experiment with **12** monitored by thin layer chromatography established that a quantitative conversion to the open VHF form upon

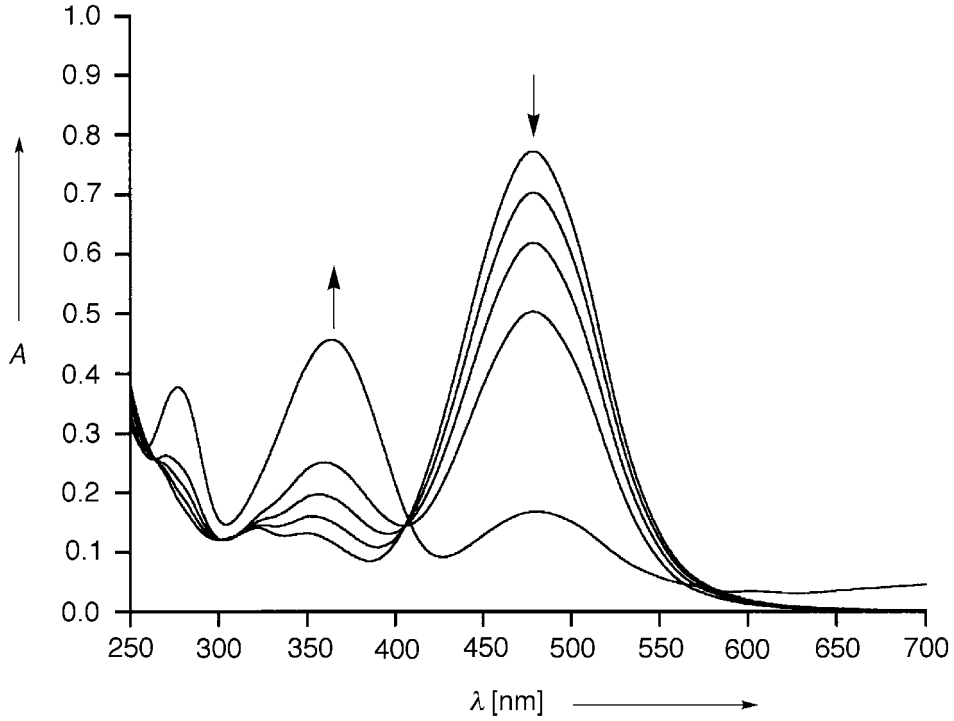

Fig. 7. *UV/VIS Spectra recorded during the thermal electrocyclization of* **4** *in* CH_2Cl_2 ($c = 2.33 \cdot 10^{-5}$ M) *at 27°*. Spectra recorded after 0, 52, 112, 232, and 1227 min.

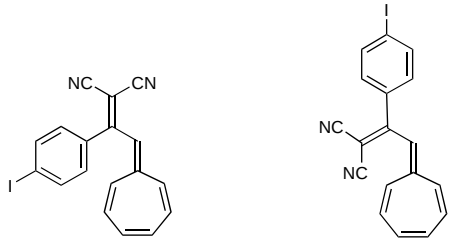

s-*trans*-**4** s-*cis*-**4**

Fig. 8. *s*-trans- *and s*-cis-*Conformations of* **4**. The thermal electrocyclization to **1** proceeds *via* the s-*cis*-conformation. In the crystal, **4** presumably adopts the s-*trans*-conformation and, hence, is thermally stable up to the melting point temperature.

irradiation at 366 nm did not take place. The reason for this lies in the thermal VHF → DHA back reaction. The position of the photoequilibrium between the two species depends strongly on the experimental conditions, thus quantification was not possible. The thermal back reaction was studied for all TEE-VHF conjugates in CH_2Cl_2 solution

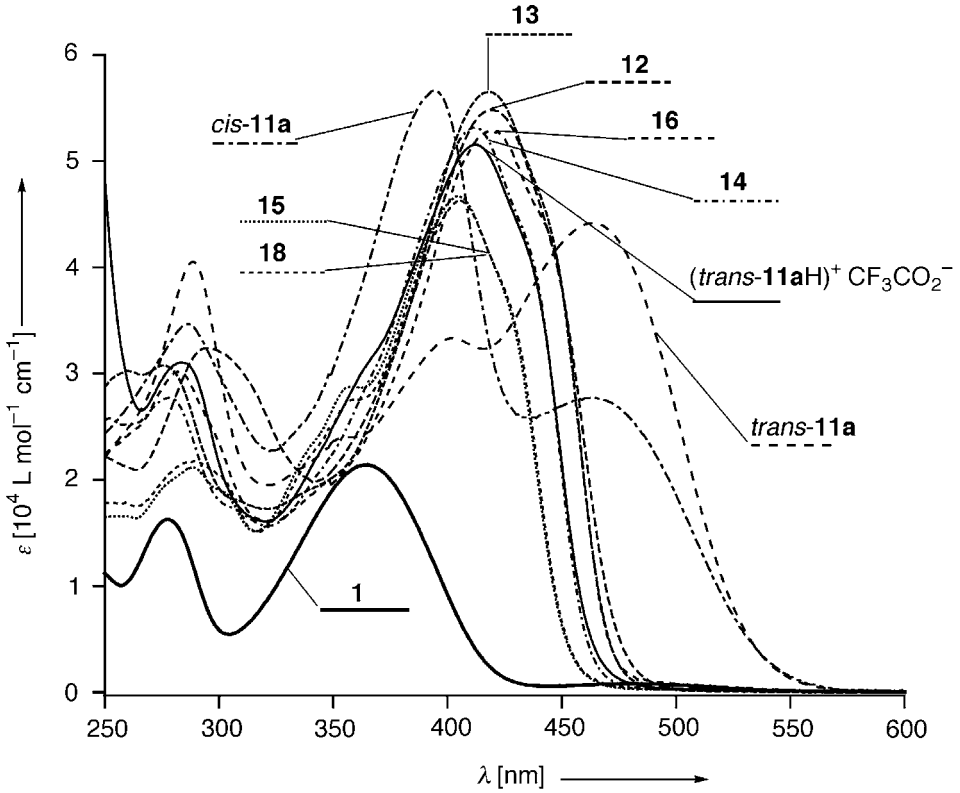

Fig. 9. *Electronic absorption spectra of the TEE-DHA conjugates recorded at room temperature in CH_2Cl_2.* Also shown for comparison is the spectrum of **1**.

at room temperature. Monitoring this process by UV/VIS spectroscopy is illustrated in *Fig. 13* for the conversion **21** → **18**, during which the VHF band at 481 nm faded away, while the DHA band at 405 nm increased in intensity.

The rate constants for the thermal electrocyclization VHF → DHA in the various hybrid systems, $k_{25°}$, and the half-life times, $t_{1/2}$, were calculated by monitoring the absorption at a defined wavelength as a function of time and exponential fitting of the resulting curves (*Table 3*). For all VHF-TEE systems, with the exception of the protonated DMA derivatives (*cis*-**11a**H)$^+CF_3CO_2^-$ (=*cis*-**11b**; *cf. Scheme 9*) and (*trans*-**11a**H)$^+CF_3CO_2^-$ (=*trans*-**11b**; *cf. Scheme 9*), very similar values were obtained in CH_2Cl_2, with $t_{1/2}$ ranging between 4.3 and 5.0 h. Correspondingly, linearization of the kinetic data afforded parallel lines (*Fig. 14*). Also, the end-absorption wavelengths of the VHF isomers of **12**–**16** and **18** (between 473 and 481 nm) are very similar to the value measured for **4** (478 nm). These data, together with the similarity of the UV/VIS spectra shown in *Fig. 9*, suggest that, in these conjugates, the DHA/VHF group on one side of the central TEE core perceives only weakly the nature of the substituent on the other. The comparison between the half-life times of **4** (5.8 h) and the TEE hybrid derivatives shows a small increase in the rate of the thermal electrocyclization reaction.

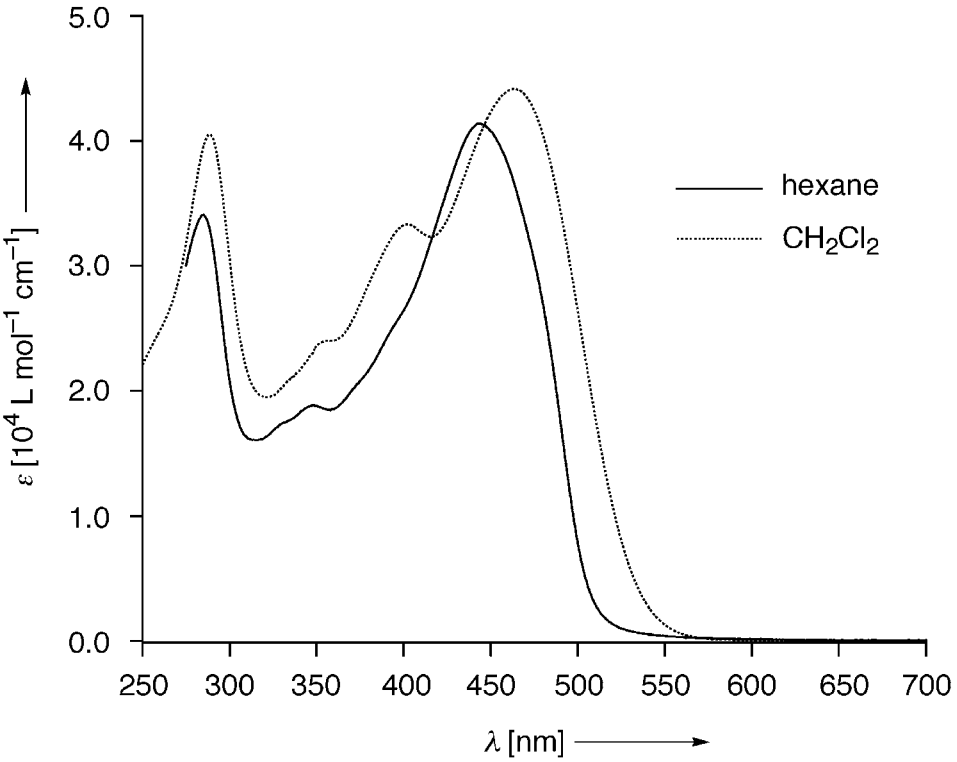

Fig. 10. *Electronic absorption spectra of* trans-**11a** *in hexane* ($c = 1.73 \cdot 10^{-5}$ M) *and* CH_2Cl_2 ($c = 1.70 \cdot 10^{-5}$ M) *at room temperature*

Table 2. *Maxima and Molar Extinction Coefficients of the Longest-Wavelength Absorption Bands of DHA Derivatives in* CH_2Cl_2

Compound	Substituent	λ_{max} [nm]	ε [$l \cdot mol^{-1} \cdot cm^{-1}$]
1	–	365	21400
trans-**11a**	4-$Me_2N-C_6H_4$	402/464	33300/44200
trans-**11b** [a])	4-$Me_2HN^+-C_6H_4$	412	51600
cis-**11a**	4-$Me_2N-C_6H_4$	394/464	56600/27800
12	4-$O_2N-C_6H_4$	419	54800
13	4-$MeO-C_6H_4$	419	56500
14	C_6H_5	412	53200
15	Me_3Si	404	46700
16	2-Thienyl	420	51300
18	(i-Pr)$_3$Si	406	46300

[a]) *trans*-**11b** = (*trans*-**11a**H)$^+CF_3CO_2^-$; see *Scheme 9*.

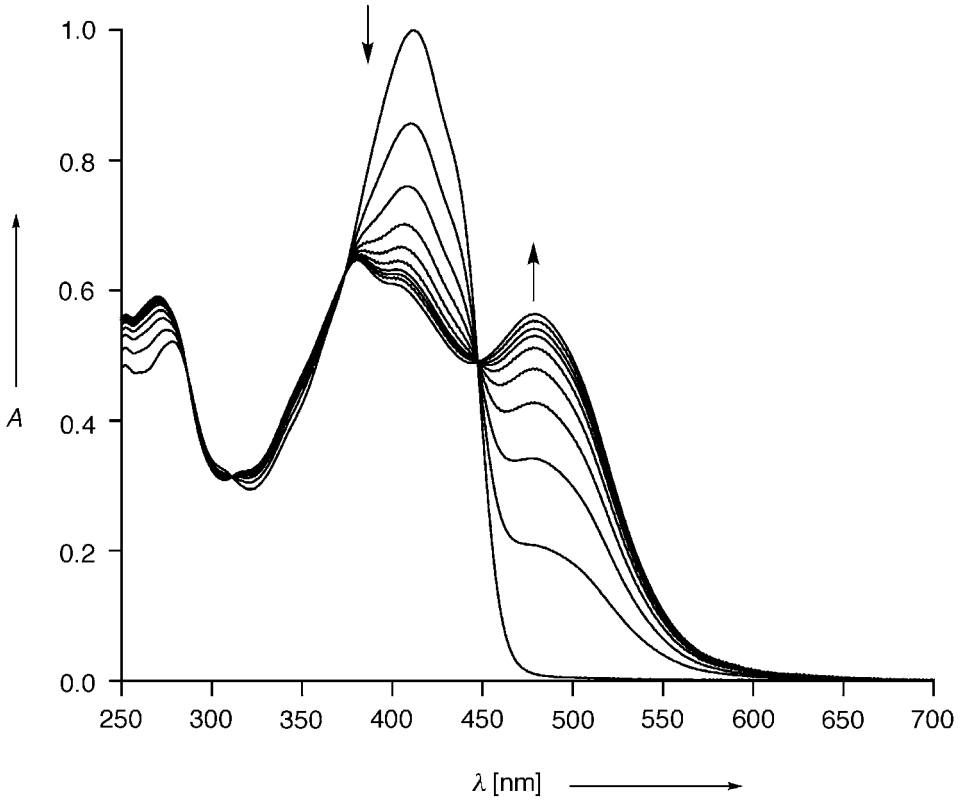

Fig. 11. *Photochromism of TEE-DHA hybrid derivative* **14** *in* CH_2Cl_2 ($c = 1.88 \cdot 10^{-5}$ M) *after irradiation at 366 nm*. Spectra recorded after 0, 15, 30, 45, 60, 75, 90, 105, 120, 180, and 480 s.

This increase can be readily explained with the π-electron-acceptor properties of the TEE core [27], as previous studies by *Daub et al.* had shown that the VHF → DHA isomerization in arylated derivatives (such as **1**/**4**) is slightly accelerated by electron-withdrawing *para*-substituents on the aryl ring [18a].

The 16-times higher electrocyclization rate constant of the protonated DMA derivative most probably finds its origin in the polar environment arising from the addition of CF_3COOH. In a control experiment, 20 µl of CF_3COOH was added to a solution of **18** in CH_2Cl_2 (3 ml), which represents the amount of acid used in standard experiments to protonate *trans*-**11a** or *cis*-**11a**. The sample was irradiated at 405 nm, and the cyclization **21** → **18** was subsequently monitored at 481 nm (*Fig. 15*). A remarkably enhanced rate constant $k_{25°} = 2.7 \cdot 10^{-4}\ s^{-1}$ ($t_{1/2} = 43$ min) was measured in the presence of the acid. The stabilization of the postulated [28] highly polar transition state of the VHF → DHA electrocyclization process through the presence of CF_3COOH could account for these observations.

2.4. *A Three-Way Chromophoric Molecular Switch*. Among the DHA/VHF switching experiments described in *Sect. 2.3*, the non-protonated conjugates *trans*-**11a** and *cis*-**11a** are notably absent. In fact, these compounds were also included in the

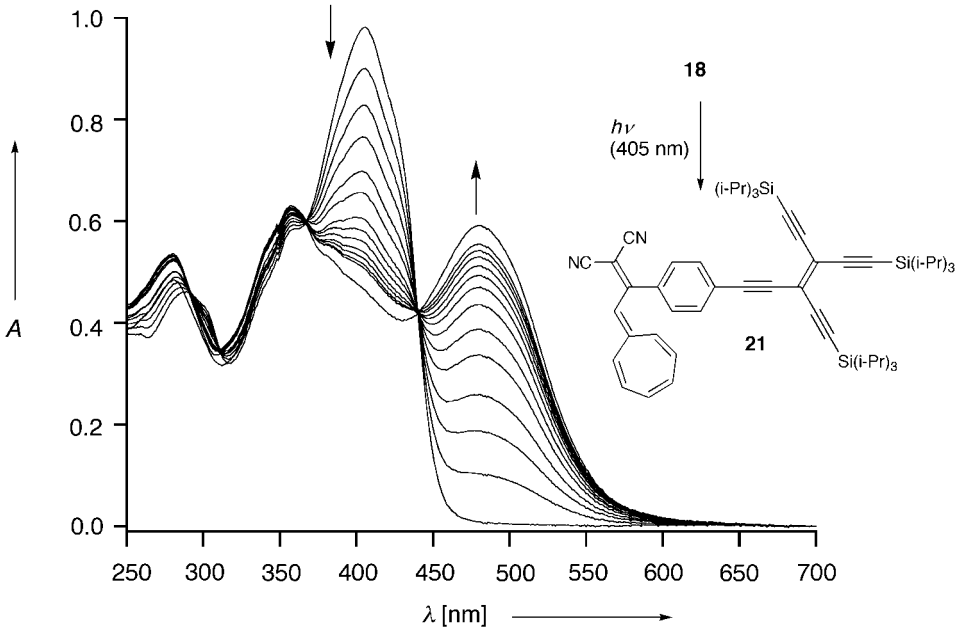

Fig. 12. *Electronic absorption spectra in CH_2Cl_2 ($c = 2.12 \cdot 10^{-5}$ M, $T = 25°$) recorded in 30-s intervals during the photoisomerization of* **18** *to* **21**. Last spectrum recorded after 11 min. $\lambda_{irr} = 405$ nm.

investigation, but it rapidly became clear that the switching process could not be observed or did not take place. When we found, however, that rapid switching occurred upon protonation of the DMA residue, we had discovered a new three-way chromophoric molecular switch (for a report on a three-way switch consisting of a DHA group and an acid-sensitive, redox-active anthraquinone moiety, see [29]). The three addressable sub-units in **11**, capable of undergoing individual, reversible switching cycles are *i*) the TEE core, which can be reversibly photoisomerized between its *cis*- and *trans*-forms, *ii*) the DHA unit, which can be transformed into a VHF moiety upon irradiation, and *iii*) the proton-sensitive DMA group. With three possible switching processes, **11** can adopt eight interconvertible states. Such a complex system is best visualized in a three-dimensional representation by a cube with each corner describing one distinct state (*trans*-**11a**–**d** and *cis*-**11a**–**d**; *Scheme 9*). Despite this functional complexity, individual interconversion processes could be cleanly addressed and six of the eight states were detected.

As a first function of this highly programmed molecular system, we investigated the photochemical *trans/cis*-isomerization of the central TEE core. Irradiation at the longest-wavelength absorption maximum ($\lambda_{max} = 464$ nm, $\varepsilon = 44000\,l \cdot mol^{-1} \cdot cm^{-1}$) of *trans*-**11a** induced rapid conversion to *cis*-**11a**, while irradiating into the most intense absorption band of the latter ($\lambda_{max} = 396$ nm, $\varepsilon = 55000\,l \cdot mol^{-1} \cdot cm^{-1}$) allowed the reverse reaction to take place (*Fig. 16*). The ratio of *trans*- and *cis*-isomers at the photostationary states and the quantum yields for the photoisomerization processes are summarized in *Table 4*.

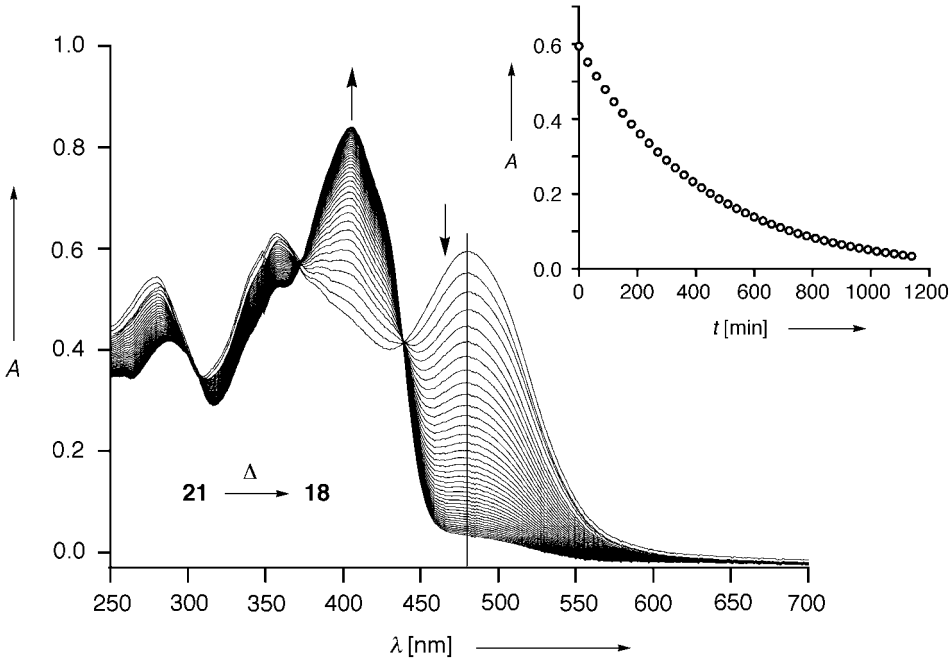

Fig. 13. *Electronic absorption spectra recorded in 30-min intervals in CH_2Cl_2 ($c = 2.12 \cdot 10^{-5}$ M) at 25° during the thermal isomerization of* **21** *to* **18**. The time-dependent decrease of the absorption at 481 nm is represented in the top right corner. The rate constant, $k_{25°}$, and the half-life time, $t_{1/2}$, were determined by an exponential fit to these data.

Table 3. *Half-Life Times,* $t_{1/2}$, *and Rate Constants,* $k_{25°}$, *of the Thermal Reactions VHF → DHA in CH_2Cl_2 at 25° and the Longest-Wavelength Absorption Maxima,* λ_{max} (starred), *of the VHF Isomers.* If the wavelength used for the kinetic evaluation differed from λ_{max}, both wavelengths are given.

DHA	$t_{1/2}$ [h]	k [10^{-5} s^{-1}]	λ_{max} [nm]
12	4.5	4.3	481*
13	4.8	4.0	500 (473*)
14	4.8	4.0	480*
15	5.0	3.9	481*
16	4.5	4.3	500 (474*)
18	4.3	4.5	481*
trans-**11b** [a])	0.26	73.7	500*

[a]) *trans*-**11b** = (*trans*-**11a**H)$^+CF_3CO_2^-$; see *Scheme 9*.

Both *cis*-**11a** and *trans*-**11a** displayed a strong fluorescence with a maximum at $\lambda =$ 606 nm. This emission was monitored during several switching cycles to study the resistance of the *trans/cis* isomerization process to photofatigue (*Fig. 17*). After 15 cycles, the intensity of the fluorescence at 606 nm decreased to about 90% of the initial value.

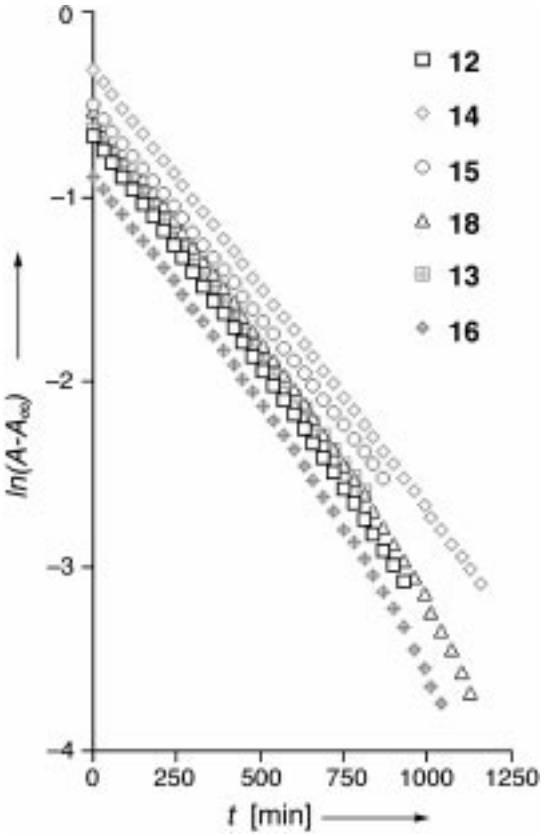

Fig. 14. *Linearized representation of the decrease of the VHF absorption band during the thermal VHF → DHA isomerization process in CH_2Cl_2 at 25°.* For the wavelength of the measurements, see *Table 3*.

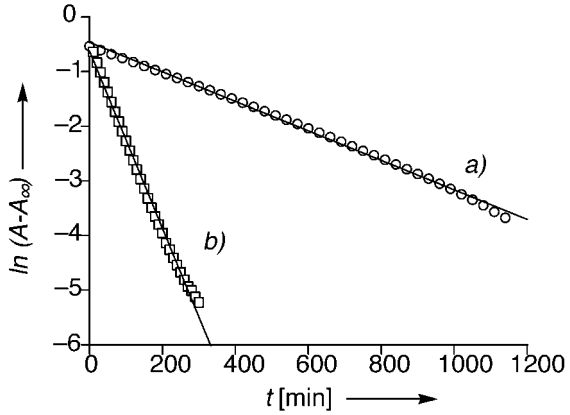

Fig. 15. *Addition of CF_3COOH leads to an increase of the rate constant for the electrocyclization* **21** → **18**. For the reaction in pure CH_2Cl_2 *a*) $k_{25°} = 4.5 \cdot 10^{-5}$ s^{-1} ($t_{1/2} = 4.3$ h). For the reaction in CH_2Cl_2 (3 ml) + CF_3COOH (20 µl) *b*) $k_{25°} = 2.7 \cdot 10^{-4}$ s^{-1} ($t_{1/2} = 43$ min). Absorbances collected at 281 nm; (c(**21** + **18**) $= 2.12 \cdot 10^{-5}$ M).

Scheme 9. *Three-Dimensional Switching Diagram of TEE-DHA Hybrid Derivative* **11**. The eight possible states are shown as the corners of a cube. $CF_3CO_2^-$ is the counterion of **11b** and **11c**.

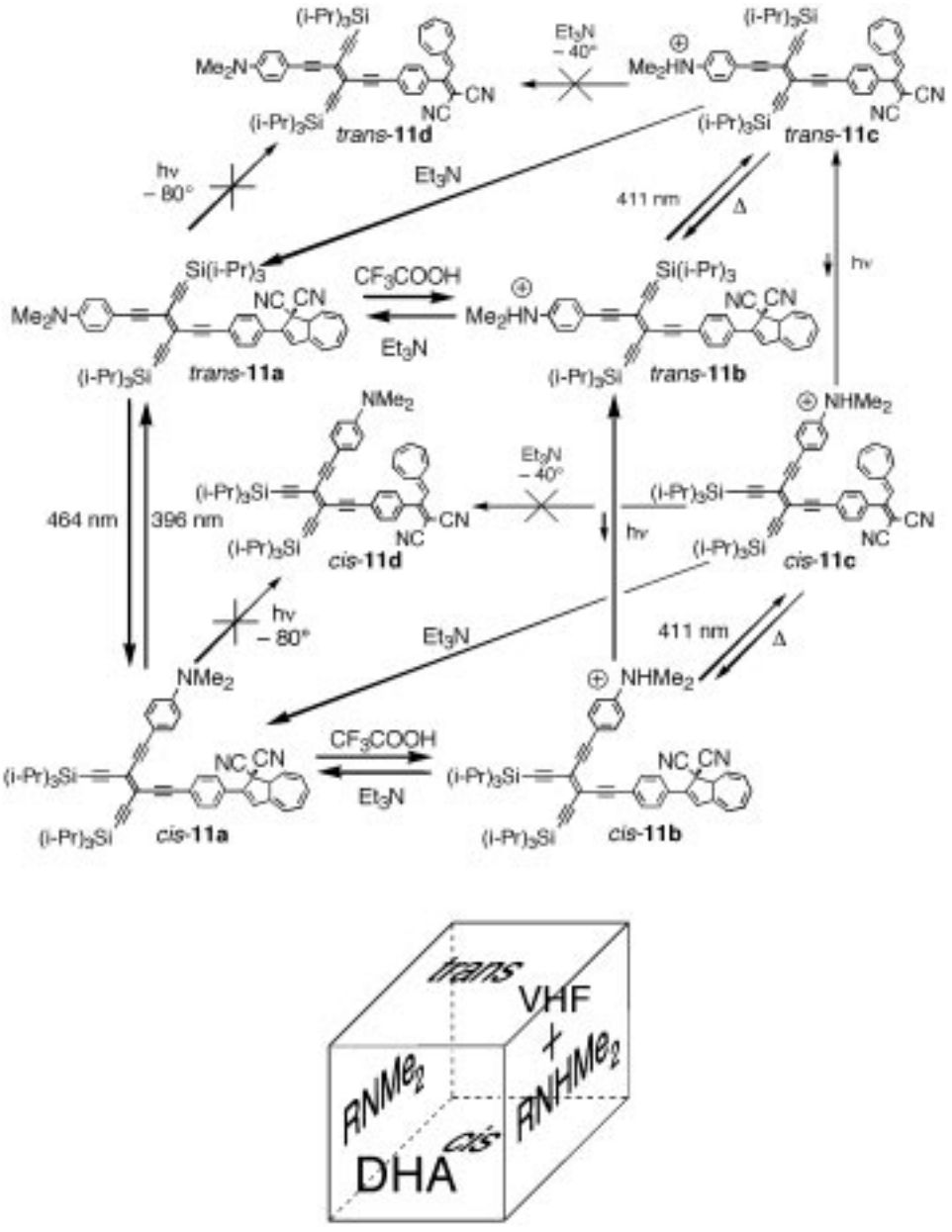

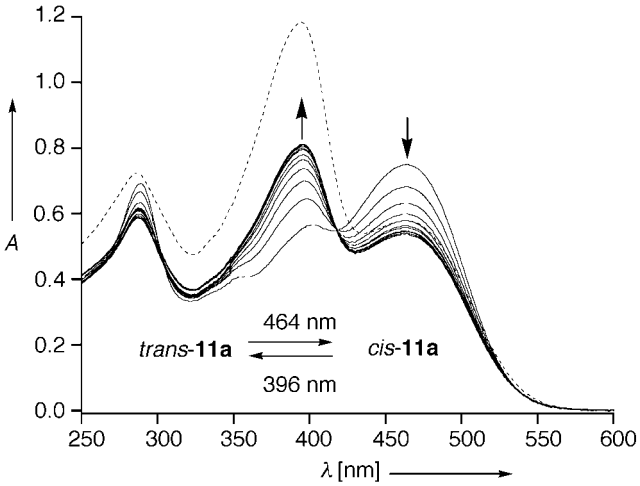

Fig. 16. *Electronic absorption spectrum of pure* cis-**11a** *in* CH_2Cl_2 (----, $c = 2.12 \cdot 10^{-5}$ M) *and spectra recorded every 10 s during the* trans → cis *isomerization* ($\lambda_{irr} = 464$ nm), *starting from pure* trans-**11a** (—, $c = 1.70 \cdot 10^{-5}$ M)

Table 4. *Physical Data for the Photochemical* trans/cis-*Isomerization between* trans-**11a** *and* cis-**11a** *in* CH_2Cl_2 *at 25°*

λ[a]) [nm]	% *cis* [b])	% *trans* [b])	$\Phi_{c\to t}$[c])	$\Phi_{t\to c}$[c])	K_{eq}[d])	ε_{cis}[e]) [l · mol^{-1} · cm^{-1}]	ε_{trans}[e]) [l · mol^{-1} · cm^{-1}]
396	35	65	0.19	0.17	1.83	55000	33000
464	68	32	0.51	0.37	2.15	26000	44000

[a]) Irradiation wavelength.
[b]) Percentage of *cis*-**11a** and *trans*-**11a**, respectively, in the photostationary state.
[c]) Partial quantum yields for the *cis* → *trans* and *trans* → *cis* interconversions, respectively (the quantum yield determination is described in [17]).
[d]) Photoequilibrium constant, *i.e.*, the ratio [product isomer]/[starting isomer] at the photostationary state.
[e]) Molar extinction coefficients of *cis*-**11a** and *trans*-**11a** at the irradiation wavelength.

This clean monitoring of the *trans/cis*-photoisomerization between *trans*-**11a** and *cis*-**11a** was possible since the photoinduced retrocyclization of these hybrid derivatives to the isomeric VHF forms *cis*-**11d** and *trans*-**11d** (*Scheme 9*) could not be accomplished, as mentioned in the introduction to this *Sect.* However, when the DMA moiety in **11a** was protonated with CF_3COOH – leading to **11b** (*Scheme 9*) – the photochemical ring opening to the isomeric VHF form **11c** took place. Protonation of **11a** to give **11b** is clearly indicated by the downfield shifts of the aromatic ^{1}H-NMR signals of the DMA group (from 6.65 and 7.39 ppm to 7.51 and 7.65 ppm for the *trans*-isomer, and from 6.67 and 7.38 ppm to 7.51 and 7.62 ppm for the *cis*-isomer). Yellow solutions of protonated DHA derivatives *cis*-**11b** and *trans*-**11b** in CH_2Cl_2 both showed absorption maxima of similar intensities at 411 nm and displayed only a weak yellow fluorescence. The VHF-containing compounds *cis*-**11c** and *trans*-**11c** featured new absorption band at $\lambda_{max} = 500$ nm, which renders the solution orange-brown. The

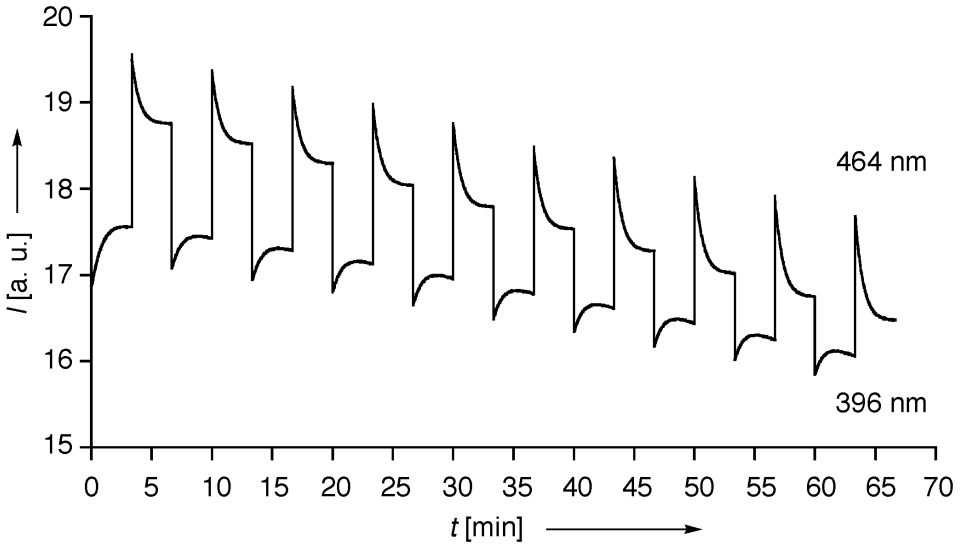

Fig. 17. *Intensity of the fluorescence of* **11a** *in* CH_2Cl_2 ($c = 2.12 \cdot 10^{-5}$ M) *recorded at 606 nm and 25° for 10 switching cycles starting from* cis-**11a**. The sample was irradiated at 396 nm (*cis*-**11a** → *trans*-**11a**) and at 464 nm (*trans*-**11a** → *cis*-**11a**).

conversion of *trans*-**11b** to *trans*-**11c**, upon irradiation at $\lambda = 411$ nm, was monitored both by ^{1}H-NMR (*Fig. 18*) and UV/VIS (*Fig. 19*) spectroscopy. Standard ^{1}H-NMR solutions ($c \approx 10$ mM) of *trans*-**11b** are too concentrated to be irradiated and successfully switched. Diluted solutions, however, can be switched at low temperature ($-50°$), which must also be maintained during the recording of the ^{1}H-NMR spectra in order to prevent thermal VHF → DHA back reaction during data acquisition time. Thus, when a dilute solution ($c \approx 0.3$ mM) of *trans*-**11b** in $CDCl_3$ in a NMR tube was irradiated at 411 nm at $-50°$, the DHA → VHF conversion could be nicely observed by ^{1}H-NMR spectroscopy. The resonances of both DHA and VHF isomers were readily discernable in the spectra (*Fig. 18*), and the absence of any non-assignable peaks demonstrated the clean isomerization between the two forms. The VHF derivative **11c** (*trans* or *cis*) readily undergoes thermal electrocyclization back to **11b** ($k_{25°} = 7.37 \pm 0.02 \cdot 10^{-4}$ s^{-1}, $t_{1/2} = 15.7$ min); therefore, mixtures of **11b** and **11c** are always observed, even after long irradiation times at room temperature. The ratio of the DHA and VHF isomers at equilibrium proved to be strongly dependent on the experimental conditions; in the NMR experiment (*Fig. 18*) the final ratio of *trans*-**11c** to *trans*-**11b** was *ca.* 90 : 10.

The clean *trans*-**11b** → *trans*-**11c** interconversion during irradiation at the specific wavelength of 411 nm, without any isomerization to the *cis*-forms, was also evidenced by several isosbestic points in the UV/VIS spectra (*Fig. 19*). At other wavelengths, *trans* → *cis* isomerization also occurred.

Treatment of **11c** (a mixture of *cis*- and *trans*-isomers) with Et_3N causes deprotonation of the amino group and leads directly to the formation of the DHA-containing compound **11a**, as observed by UV/VIS, and ^{1}H- and ^{13}C-NMR spectro-

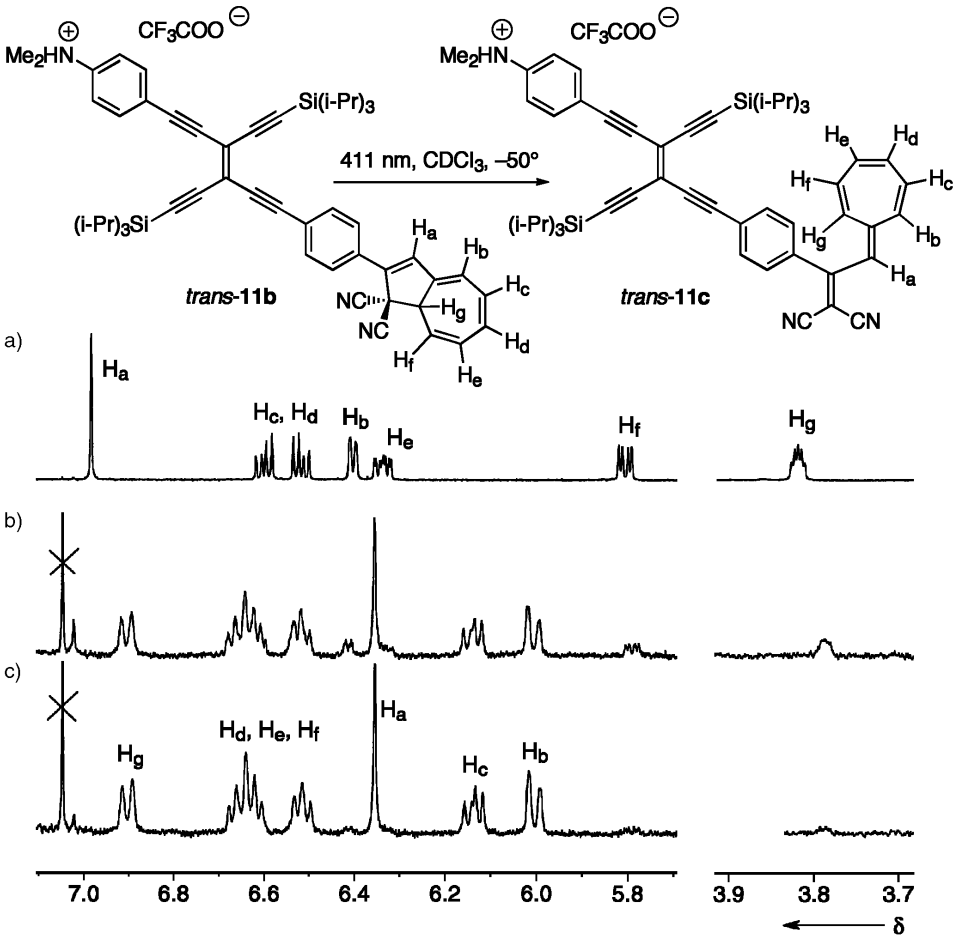

Fig. 18. *Characteristic ^{1}H-NMR signals recorded during* trans-**11b** → trans-**11c** *isomerization in* $CDCl_3$. *a*) DHA Isomer *trans*-**11b** at 0° ($c = 1.44 \cdot 10^{-2}$ M). *b*) After 2 h irradiation at 411 nm and −50° ($c = 3 \cdot 10^{-4}$ M). *c*) After 4.5 h irradiation at 411 nm and −50° ($c = 3 \cdot 10^{-4}$M). The latter spectrum mainly shows the resonances of the VHF isomer with *ca.* 10% remaining DHA isomer. The signal around 7.10 ppm is a satellite peak from $CDCl_3$ in the very dilute solution.

scopy. The VHF-containing donor-acceptor system **11d** could be obtained neither by deprotonation of **11c** – even at −40° – nor by irradiation of the DMA derivative **11a** at −80°. These results are tentatively attributed to a very fast thermal electrocyclization of any intermediately formed **11d** to **11a**.

The addition of Et_3N is not responsible for the extremely fast back reaction of **11d**: in a control experiment, a solution of **18** was irradiated, giving **21**, which, after addition of Et_3N, did not show a faster thermal isomerization than in the absence of the base (*Fig. 13*). Although the presence of the strongly electron-donating DMA substituent in **11** is clearly associated with the failure to observe the VHF-form **11d**, its role is not

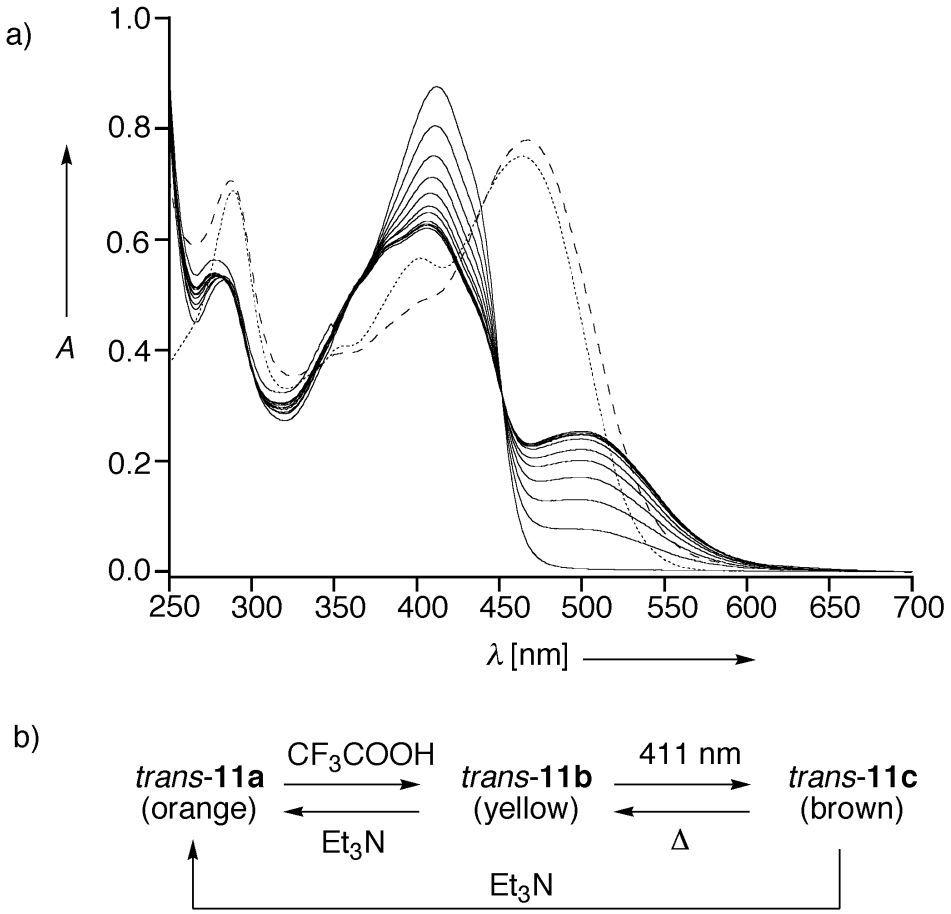

Fig. 19. a) *Electronic absorption spectra for the switching process* trans-**11a** → trans-**11b** → trans-**11c** → trans-**11a**. b) *in* CH_2Cl_2 ($c = 1.70 \cdot 10^{-5}$ M) *at 25°*. The dotted line (·····) represents the starting material *trans*-**11a**. The solid lines (——) show the conversion *trans*-**11b** → *trans*-**11c**, recorded at 1-min intervals during the irradiation at $\lambda = 411$ nm. The dashed line (------) shows the spectrum of *trans*-**11a**, recovered after deprotonation with Et_3N.

readily explainable. Indeed, it has been reported that a simple DMA-substituted DHA (2-(4-*N*,*N*-dimethylanilino)-8a*H*-azulene-1,1-dicarbonitrile) photoisomerizes in the usual manner to give the corresponding VHF form [18a].

Beside the fast electrocyclization of **11d** to **11a**, photoinduced electron transfer (PET) or electronic energy-transfer processes (EET), which have been widely used to construct photoionically-driven fluorescent sensors and switches [30], seem also to play a role in the failure to reach the VHF state **11d**. Compounds *trans*-**11a** and *cis*-**11a** display a very intense, solvent-dependent fluorescence, and extensive experimental and computational analysis (to be published elsewhere [31]) indicates that these compounds, upon photoexcitation, prefer relaxation *via* twisted intramolecular charge-transfer states (TICT states) [32][33].

When a solution of pure *trans*-**11a** in CH_2Cl_2 was treated with CF_3COOH, then irradiated at 411 nm, and finally Et_3N was added in the dark, only *trans*-**11a** was recovered as shown by UV/VIS (*Fig. 19*) and ^{13}C-NMR spectral analysis; no trace of diastereoisomeric *cis*-**11a** could be detected. The reversible conversion of *trans*-**11a** into *trans*-**11b** and then into *trans*-**11c** can be described as a model process for an AND logic gate in electronics [3]. The *trans*-**11c** state can be obtained only when both protons and light are present; *i.e.*, two inputs are necessary to generate one output. Nondestructive readout of this 'AND' logic gate is ensured by monitoring the appearance of the absorption band of *trans*-**11c** at $\lambda_{max} = 500$ nm (*Fig. 19*). In contrast, the same cycle, starting from pure *cis*-**11a**, leads to the recovery of an isomeric mixture, containing mainly the *trans*-form, and thus the conversion *cis*-**11a** → *cis*-**11b** → *cis*-**11c** is not suited for an 'AND' logic gate, as *cis* → *trans* isomerization also occurs.

In addition to the described 'AND' logic gate, three write/erase processes are present in system **11** that are not affected by side reactions to other states on the cubic switching diagram when appropriate conditions are used: *i*) the reversible *cis/trans*-photoisomerization between *trans*-**11a** and *cis*-**11a**, and *ii*) and *iii*) the reversible protonations/deprotonations of the couples *trans*-**11a/b** and *cis*-**11a/b**. Since the fluorescence enhancement after deprotonation of **11b** amounts to a factor of *ca.* 300, a very efficient nondestructive readout of information for the *cis*-**11a/b** and *trans*-**11a/b** couples is available by using excitation light of 396 nm for the *cis* and of 464 nm for the *trans*-isomer. The fluorescence enhancement factor is very high in comparison to literature values. Systems with values over 1000 are known, but are very rare [34].

2.5. *Electrochemistry.* Cyclic voltammetry (CV) and linear-sweep voltammetry (LSV) measurements were performed in CH_2Cl_2 in the presence of 0.1M Bu_4NPF_6 (*Table 5*) with the ferrocene/ferricinium (Fc/Fc^+) redox couple as a reference.

DHA Form **1** undergoes only irreversible reactions in both CV and LSV. The first reduction takes place at -1.97 V and the oxidation at $+1.16$ V. In contrast, the VHF isomer **4** is much more readily reduced (-1.47 V) and oxidized ($+0.84$ V). The electron-withdrawing properties of the dicyanovinylene moiety in **4** explain the facilitated reduction, while the formation of an aromatic tropylium ion accounts for the easier oxidation (for previous electrochemical measurements on DHA derivatives, see [35]).

All TEE-DHA hybrid compounds, with the exception of the nitrophenyl derivative **12**, undergo first a quasi-reversible or non-reversible reduction step between -1.6 and -1.8 V, that is centered on the photoactive DHA moiety. The conjugates are reduced at *ca.* 300 mV more anodic potential than **1**, which is readily explained by the electron-withdrawing properties of the DHA-appended TEE group. With the exception of DMA derivative *trans*-**11a**, all TEE-DHA conjugates undergo a first oxidation step at *ca.* $+1.10$ V. This corresponds to a small cathodic shift of *ca.* 80 mV (compared to **1**) and is against expectations, considering the electron-withdrawing properties of the TEE moiety. However, the irreversible oxidations avoid any direct comparison of redox potentials and could therefore explain the observed potential shifts.

The first reduction step in compound **12** occurs at -1.37 V and is centered on the nitrophenyl moiety. This potential corresponds to those of related 4-nitrophenyl substituted TEE derivatives [27]. Similarly, the reversible, DMA-centered oxidation of *trans*-**11a** at $+0.40$ V is in the range of the values measured for other DMA-substituted TEEs [27]. The DMA-centered oxidation, therefore, is easier to perform than the one

Table 5. *Cyclic Voltammetry (CV) and Linear-Sweep Voltammetry (LSV) Data Measured in CH_2Cl_2 + 0.1M Bu_4NPF_6.* All potentials *vs.* Fc/Fc^+. Values shown in italics correspond to redox potentials of remaining DHA starting material in the VHF isomer obtained by photoisomerization.

Starting material	DHA					VHF				
	CV			LSV		CV			LSV	
	E° [a]) [V]	ΔE_p [b]) [mV]	E_p [c]) [V]	$E_{1/2}$ [d]) [V]	Slope [e]) [mV]	E° [a]) [V]	ΔE_p [b]) [mV]	E_p [c]) [V]	$E_{1/2}$ [d]) [V]	Slope [e]) [mV]
1			−1.97	−1.97	74			−1.47	−1.48	111
			−2.07							
			+1.16	+1.18	135			+0.87	+0.84	60
trans-**11a**	−1.80	130		−1.83	60					
	−1.94	55		−1.99	65					
	+0.40	80		+0.40	60					
				+1.00	75					
12	−1.37	70		−1.39	75	−1.38	70		−1.41	90
	−1.55	70		−1.57	60	−1.65	80		−2.06	125
			−2.04			+0.84	60		+0.86	60
				+1.08	75					
13			−1.76	−1.58	180			−1.42	−1.56	150
			−1.92					*−1.77*		
			+1.05	+1.00	75			*−1.92*		
								+0.85	+0.95	
14	−1.69	60		−1.71	60			−1.37		
			−1.85	−1.89	60	−1.69	80			
			−2.28					*−1.82*		
			+1.07	+1.08	70			*−2.27*		
			+1.37	+1.44				+0.82		
								+1.06		
15	−1.71	95		−1.75	73	*−1.34*	93		−1.38	65
			−1.89	−1.93	70	*−1.71*	96		−1.76	75
			+1.15	+1.10	80	*−1.84*	80		*−1.93*	80
						+0.82	110		+0.83	60
								+1.13	*+1.11*	96

[a]) Formal redox potential $E^\circ = (E_{pa} + E_{pc})/2$. [b]) $\Delta E_p = E_{ox} - E_{red}$ (at $\nu = 100$ mV s^{-1}), where subscripts ox and red refer to the conjugated oxidation and reduction steps, respectively. [c]) Peak potential E_p for irreversible electron transfer at $\nu = 100$ mV s^{-1}. [d]) Half-wave potential $E_{1/2}$. [e]) Slope of the linearized plot of E *vs.* $\log[I/(I_{lim} - I)]$.

of the photoactive DHA moiety. A DHA-ferrocene conjugate has previously been reported that is also oxidized first at the ferrocene moiety rather than at the photoactive DMA moiety. Interestingly, this compound, similar to *trans*-**11a**, does not photoisomerize to the VHF compound [35b].

The solutions of the TEE-DHA conjugates *trans*-**11a** and **12**–**15** were irradiated at 365 nm and the electrochemical data of the corresponding VHF forms measured. As the conversion to the VHF isomers was not complete, weak signals corresponding to the reduction steps of the DHA starting materials remained in some of the cyclic and linear-sweep voltammograms (potentials shown in italics in *Table 5*). As expected from the findings for **4**, reversible reduction steps were observed at a more positive potential compared to the DHA forms, while the oxidations take place at more negative

potential. Considering these observations, the DHA/VHF moiety can be described as a photoswitchable π-electron acceptor. In the CV measured upon irradiation of the nitrophenyl derivative **12**, the first reduction potential at -1.38 V corresponds to the overlapped signals resulting from the reversible reduction of the nitrophenyl group and the irreversible reduction of the VHF moiety.

No data are available for *trans*-**11b** as only poorly resolved voltammograms were obtained after addition of CF_3COOH to *trans*-**11a**.

A series of spectroelectrochemical measurements on solutions of **1** and **15** was performed in the dark to explore whether the ring opening of the DHA moiety to give the VHF form can be forced by electrochemical oxidation or reduction. All redox steps were irreversible in accordance with the CV measurements. The final spectra were always different from the starting ones, but evidence for an electrochemical ring opening of the DHA moiety could not be obtained. For compound **1**, electronic absorption spectra with isosbestic points and a new longest-wavelength absorption band at $\lambda_{max} = 482$ nm were recorded during the oxidation process (*Fig. 20*). Despite the similarity between the spectrum obtained upon oxidation and the one measured for VHF isomer **4** (*Fig. 6*), the newly formed species lacks the electrochemical character-

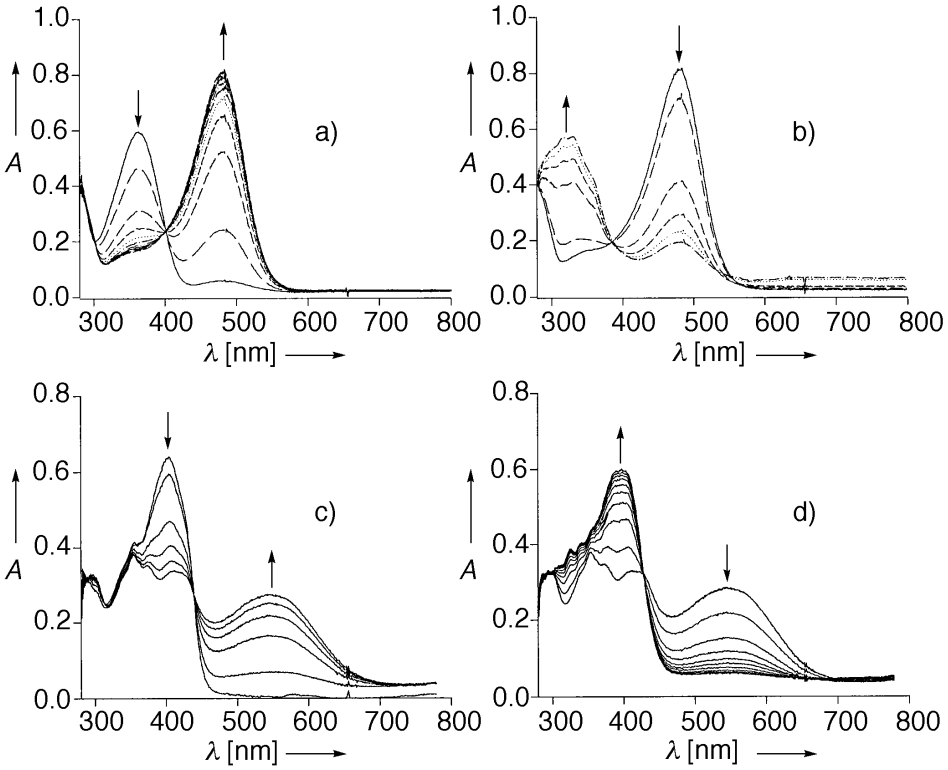

Fig. 20. *Spectroelectrochemical measurement in CH_2Cl_2. a*) Oxidation of **1** at $+1.55$ V and *b*) reduction of the so-obtained species at 0 V. *c*) Oxidation of **15** at $+1.6$ V and *d*) reduction of the so-obtained species at 0 V. Potentials given *vs.* Ag/AgCl.

istics of a VHF derivative. Also in the case of **15**, an electrochemical DHA → VHF ring opening did not take place. There exists, indeed, no precedence for such a process in the literature.

3. Conclusions. – This paper describes the synthesis, X-ray structural characterization, and exploration of the photophysical and electrochemical properties of a novel series of molecular photoswitches based on TEE-DHA hybrid systems. The DHA → VHF photoisomerization and the corresponding thermal back reaction in these conjugates were found to be much faster than the fully light-driven *trans/cis*-isomerization of the TEE moiety. The electrochemical studies clearly demonstrated that the DHA/VHF chromophore is a photoswitchable π-electron-acceptor moiety. Attempts to achieve the DHA → VHF *retro*-electrocyclization by electrochemical oxidation or reduction were not successful. Most of the TEE-DHA hybrid systems discussed in this paper (**1**, **12**–**16**, **18**) represent simple molecular devices with the ability to perform a basic write/erase process with convenient optical readouts. On the other hand, DMA derivative **11** is an example of a complex, multifunctional switchable device, capable of undergoing three individual, reversible switching cycles, namely *i*) photochemical *trans/cis*-isomerization of the TEE core, *ii*) DHA → THF photoisomerization and thermal back reaction, and *iii*) reversible protonation of the DMA group. Of the eight possible states, six were detected and several individual interconversion processes could be cleanly addressed, providing three write/erase processes and one model for an electronic AND gate. The aim is now to incorporate these systems into macroscopic devices able to perform real-life tasks. A first step has been achieved with the reversible structuring of polymeric waveguides doped with the simple molecular photoswitch **1** [22]. We are now further exploring the potential of TEE derivatives and conjugates to function as fully light-driven molecular switches in reversible information-storage devices.

Experimental Part

General. All reactions were carried out under N_2. Solvents and reagents were reagent-grade and commercially available and used without further purification unless otherwise stated. Compounds **6**, **7**, **8** [15c], and **19** [24] were prepared according to literature procedures. THF and Et_2O were freshly distilled from sodium benzophenone ketyl. BuLi solns. in hexane were titrated with 2,4-dimethoxybenzyl alcohol in THF [36]. Evaporation *in vacuo* was conducted at H_2O-aspirator pressure. Degassing of solvents was accomplished by three freeze-thaw pump cycles. Column chromatography (CC): SiO_2-*60* (230–400 mesh, 0.040–0.063 mm) from *Fluka*. M.p.: *Büchi 510* or *Büchi B-540*, uncorrected. TLC: glass-backed *Polygram* SiO_2-*60* UV_{254} from *Macherey-Nagel*, visualization by UV light (254 or 366 nm) or with a molybdenum-stain soln. (400 ml 10% aq. H_2SO_4 soln., 20 g $(NH_4)_6Mo_7O_{24} \cdot 6\,H_2O$, 0.6 g $Ce(SO_4)_2$). UV/VIS: *Varian Cary 5 UV/VIS/NIR* spectrometer at r.t.; λ_{max} in nm (ε in $M^{-1}\,cm^{-1}$). IR Spectra (cm^{-1}): *Perkin-Elmer 1600-FT IR*. NMR Spectra: *Bruker AMX-500* or *AMX-400*, and *Varian Gemini 300* or *200* at 296 or 300 K, with solvent peak as reference. MS (*m/z* (%)); EI-MS: *VG TRIBRID* spectrometer at 70 eV; FAB-MS: *VG ZAB2-SEQ* spectrometer with 3-nitrobenzyl alcohol (NOBA) as matrix. Elemental analyses were performed by the Mikrolabor at the Laboratorium für Organische Chemie, ETH-Zürich.

Electrochemistry. CH_2Cl_2 was purchased spectroscopic grade from *Merck*, dried over molecular sieves (4 Å), and stored under Ar prior to use. Bu_4NPF_6 was purchased electrochemical grade from *Fluka* and used as received.

The electrochemical experiments were carried out at $20 \pm 2°$ in CH_2Cl_2 containing 0.1M Bu_4NPF_6 in a classical three-electrode cell. The working electrode was a glassy carbon disk electrode used either in motionless

mode for CV (10 mV s^{-1} to 10 V s^{-1}) or as rotating-disk electrode for LSV. The electrochemical cell was connected to a computerized multipurpose electrochemical device *DACFAMOV* (*Microtec-CNRS*, Toulouse, France) interfaced with an *Apple II* microcomputer. All potentials are referenced to the ferrocene/ferricinium (Fc/Fc^+) couple used as an internal standard. The auxiliary electrode was a Pt wire, and an Ag wire was used as a pseudo-reference electrode. The accessible range of potentials was +1.2 to −2.2 V *vs.* Fc/Fc^+ in CH_2Cl_2. Spectroelectrochemical measurements were performed in a thin-layer cell (0.1 mm) through an optically transparent thin-layer electrode (*OTTLE*) made of a Pt mini-grid (1000 mesh). The auxiliary electrode was a Pt wire, and an aq. Ag/AgCl electrode was used as the reference. The *OTTLE* cell was placed in a *Hewlett Packard* diode-array UV/VIS spectrometer model *8452A*. The *OTTLE* cell was connected to a *Bruker* potentiostat (model *EI30M*) for control and measurement of the electrochemical parameters.

X-Ray Crystal Structure of **1**. Crystal data at 293 K for ($C_{18}H_{11}IN_2$) (M_r 382.20): triclinic, space group $P\bar{1}$ (No. 2), $D_c = 1.679$ g cm^{-3}, $Z = 2$, $a = 9.243(2)$, $b = 9.519(2)$, $c = 10.527(3)$ Å, $\alpha = 73.89(2)^\circ$, $\beta = 65.77(2)^\circ$, $\gamma = 64.35(2)^\circ$, $V = 755.7(3)$ Å^3. *Syntex P21* diffractometer, MoK_α radiation, $\lambda = 0.71073$ Å. The structure was solved by direct methods (SHELXTL PLUS) and refined with 191 parameters by full-matrix least-squares analysis based on F^2 and experimental weights; all heavy atoms were refined anisotropically and H-atoms fixed isotropically with positions calculated from stereochemical considerations. Final $R(F) = 0.025$ for 1304 observed reflections with $I > 2\sigma(I)$ and $wR(F^2) = 0.067$ for all 1422 data. *Cambridge Crystallographic Data Centre* deposition No. CCDC-151574.

X-Ray Crystal Structure of cis-**11a**. Crystal data at 293 K for ($C_{54}H_{63}N_3Si_2$) (M_r 810.29): monoclinic, space group $P2(1)/c$ (No. 14), $D_c = 1.065$ g cm^{-3}, $Z = 4$, $a = 29.97(3)$, $b = 7.764(7)$, $c = 23.58(2)$ Å, $\beta = 113.11(6)^\circ$, $V = 5046(9)$ Å^3. *Picker-Stoe* diffractometer, CuK_α radiation, $\lambda = 1.54178$ Å. The structure was solved by direct methods (SHELXTL PLUS) and refined with 547 parameters by full-matrix least-squares analysis based on F^2 and experimental weights; all heavy atoms were refined anisotropically, H-atoms fixed isotropically with positions calculated from stereochemical considerations. Final $R(F) = 0.079$ for 2294 observed reflections with $I > 2\sigma(I)$ and $wR(F^2) = 0.215$ for all 3072 data. *Cambridge Crystallographic Data Centre* deposition No. CCDC-151573. For the X-ray crystal structure of *trans*-**11a**, see [17] and *Cambridge Crystallographic Data Centre* deposition No. CCDC-102924.

X-Ray Crystal Structure of **12**. Crystal data at 295 K for ($C_{52}H_{57}N_3O_2Si_2$) ($M_r = 812.19$): triclinic, space group $P1$ (No. 1), $D_c = 1.114$ g cm^{-3}, $Z = 1$, $a = 7.409(1)$ Å, $b = 13.608(1)$ Å, $c = 13.616(2)$ Å, $\alpha = 66.27(1)^\circ$, $\beta = 75.01(1)^\circ$, $\gamma = 87.74(1)^\circ$, $V = 1270.7(3)$ Å^3. *Nonius CAD4* diffractometer, MoK_α radiation, $\lambda = 0.7107$ Å. Single crystals were obtained by slow evaporation of a $MeCN/CH_2Cl_2$ soln. The structure was solved by direct methods (SHELXS-86) [37] and refined by full-matrix least-squares analysis (SHELXL-93) [38], with an isotropic extinction correction and $w = 1/[\sigma^2(F_o^2) + (0.143P)^2 + 0.047P]$, where $P = (F_o^2 + 2F_c^2)/3$. All heavy atoms were refined anisotropically (H-atoms isotropic, whereby H-positions are based on stereochemical considerations). Final $R(F) = 0.055$, w$R(F^2) = 0.149$ for 583 parameters, 3 restraints, and 2693 reflections with $I > 2\sigma(I)$ and $\theta < 23.96^\circ$. *Cambridge Crystallographic Data Centre* deposition No. CCDC-151798.

X-Ray Crystal Structure of **13**. Crystal data at 213 K for ($C_{53}H_{60}N_2OSi_2$) (M_r 797.21): triclinic, space group $P\bar{1}$ (No. 2), $D_c = 1.097$ g cm^{-3}, $Z = 2$, $a = 7.905(4)$ Å, $b = 16.044(7)$ Å, $c = 20.097(4)$ Å, $\alpha = 104.96(3)^\circ$, $\beta = 94.16(2)^\circ$ $\gamma = 99.28(3)^\circ$, $V = 2413(2)$ Å^3. *Nonius CAD4* diffractometer, CuK_α radiation, $\lambda = 1.5418$ Å. Single crystals were obtained by slow evaporation of a $MeCN/CH_2Cl_2$ soln. The structure was solved by direct methods (SHELXS-86) [37] and refined by full-matrix least-squares analysis (SHELXL-93) [38], with an isotropic extinction correction and $w = 1/[\sigma^2(F_o^2) + (0.163P)^2 + 4.329P]$, where $P = (F_o^2 + 2F_c^2)/3$. The six-membered ring with the MeO group (C(27) to C(34)) and the (i-Pr)$_3$Si group (Si(2) to C(45)) are disordered over two orientations. In *Fig. 5*, only one orientation is shown for clarity. The disordered atoms C(27) to C(34) were refined anisotropically with population parameters (pp) of 0.5, except that of C(34), which was set to 1.0. The disordered atoms Si(2) to C(45) were refined isotropically with pp of 0.5. The C−C bond lengths within the disordered six-membered ring were restrained to *ca.* 1.39 Å, those within the disordered (i-Pr)$_3$Si group to *ca.* 1.52 Å. The remaining heavy atoms were refined anisotropically (H-atoms of the ordered skeleton isotropically, whereby H-positions are based on stereochemical considerations). Final $R(F) = 0.093$, w$R(F^2) = 0.273$ for 597 parameters, 36 restraints, and 3538 reflections with $I > 2\sigma(I)$ and $\theta < 49.97^\circ$. *Cambridge Crystallographic Data Centre* deposition No. CCDC-151797.

Copies of the crystallographic data (excluding structure factors) for all new structures presented here can be obtained, free of charge, on application to the *Cambridge Crystallographic Data Centre,* 12 Union Road, Cambridge CB2 1EZ, UK (fax: +44(1223)336033; e-mail: deposit@ccdc.cam.ac.uk).

General Protocol for the DHA → VHF and trans-**11a**/cis-**11a** *Photoisomerizations.* The isomerization reactions in spectral-grade CH_2Cl_2 (typical concentrations $c \approx 2 \cdot 10^{-5}$ M) were executed at 25° in a 1-cm quartz

cell and the conversions monitored with a *Varian Cary 5 UV/VIS/NIR* spectrometer. The cell was irradiated with monochromatic light from a *Spex Fluorolog 1680 0.22m Double Spectrometer*. For irradiations at 366 nm, a *sterilAir BLB-8* UV lamp for the visualization of TLC plates was used, and the light was not monochromatic.

General Protocol for the VHF → DHA Electrocyclizations. The quartz cells containing the irradiated solns. were kept in the dark at 25°, and the absorption spectra were recorded at regular intervals on a *Varian Cary 5 UV/VIS/NIR* spectrometer.

*2-(4-Iodophenyl)-8a*H*-azulene-1,1-dicarbonitrile* (**1**). A soln. of tritylium tetrafluoroborate (6.09 g, 18.4 mmol) in 1,2-dichlorethane (100 ml) was added *via* cannula to **3** (6.75 g, 17.6 mmol) in 1,2-dichlorethane (25 ml) under N_2. The mixture was stirred for 1 h at 80°, then poured onto PhMe (400 ml). After cooling the red soln. to 0°, Et_3N (2.69 ml, 19.3 mmol) was added dropwise and the temp. was raised over 1 h to 20°. Finally, the mixture was stirred for 1 h at 80° under exclusion of light. CC (short plug of SiO_2-*60*; CH_2Cl_2/hexane 1:1) followed by recrystallization (hexane) afforded **1** (4.71 g, 70%). Yellow powder. M.p. 143°. UV/VIS (CH_2Cl_2): 277 (16200), 365 (21400). IR (KBr): 3056*w*, 2889*w*, 1484*m*, 1005*m*, 824*s*, 812*s*, 707*s*. ^{1}H-NMR (200 MHz, $CDCl_3$): 3.78–3.81 (*m*, 1 H); 5.82 (*dd*, *J* = 10.0, 3.7, 1 H); 6.27–6.39 (*m*, 2 H); 6.46–6.63 (*m*, 2 H); 6.91 (*s*, 1 H); 7.47 (*d*, *J* = 8.7, 2 H); 7.82 (*d*, *J* = 8.7, 2 H). ^{13}C-NMR (125 MHz, $CDCl_3$): 45.02; 51.03; 96.20; 112.51; 114.90; 119.42; 121.52; 127.60; 127.73; 129.91; 130.84; 131.19; 132.94; 138.32; 138.41; 139.05. EI-MS: 382.1 (78, M^+), 355.0 (31, $[M-HCN]^+$), 255.2 (100, $[M-I]^+$), 227.1 (71), 201.1 (27), 127.1 (12, I^+), 100.1 (33). Anal. calc. for $C_{18}H_{11}N_2I$ (382.20): C 56.57, H 2.90, N 7.33; found: C 56.56, H 2.90, N 7.36. X-Ray, see *Fig. 2*.

2-(2,4,6-Cycloheptatriene-1-yl)-1-(4-iodophenyl)ethanone (**2**). To a suspension of tropylium tetrafluoroborate (3.94 g, 22.2 mmol) in MeOH (40 ml) were added 4-iodoacetophenone (6.00 g, 24.4 mmol) and AcOH (0.8 ml), and the resulting mixture was stirred for 6 h at 20°. H_2O (200 ml) was added, and the mixture was extracted with Et_2O (3 × 150 ml). Drying of the combined org. phases ($MgSO_4$) and CC (SiO_2-*60* (700 g); CH_2Cl_2/hexane 2:1) afforded **2** (3.75 g, 50%). Yellowish, needle-shaped crystals (Et_2O). M.p. 76°. IR (KBr): 3022*w*, 3002*w*, 2889*w*, 2856*w*, 1686*s*, 1577*s*, 1390*m*. ^{1}H-NMR (200 MHz, $CDCl_3$): 2.46–2.53 (*m*, 1 H); 3.29 (*d*, *J* = 7.5, 2 H); 5.28 (*dd*, *J* = 9.5, 5.8, 2 H); 6.18–6.26 (*m*, 2 H); 6.65–6.68 (*m*, 2 H); 7.67 (*d*, *J* = 8.5, 2 H); 7.84 (*d*, *J* = 8.5, 2 H). ^{13}C-NMR (50 MHz, $CDCl_3$): 34.68; 41.22; 101.03; 125.06; 125.25; 129.48; 131.00; 136.17; 137.92; 197.98. EI-MS: 336.1 (62, M^+), 231.0 (100, $[IPhCO]^+$), 91.1 (58, $[C_7H_7]^+$). Anal. calc. for $C_{15}H_{13}OI$ (336.17): C 53.59, H 3.90; found: C 53.32, H 3.94.

[2-(2,4,6-Cycloheptatriene-1-yl)-1-(4-iodophenyl)ethylidene]propanedinitrile (**3**). *From* **2**: In a flask equipped with a *Dean-Stark* trap, **2** (1.64 g, 4.88 mmol) and malononitrile in PhMe (50 ml) were heated to reflux for 8 h while a soln. of NH_4OAc (5 g, 64.8 mmol) in AcOH (15 ml) was added portionwise. After cooling to 20° and addition of PhMe (100 ml), the mixture was extracted with H_2O (3 × 100 ml). Drying ($MgSO_4$) and CC (SiO_2-*60* (190 g); CH_2Cl_2/hexane 2:1) afforded **3** (1.42 g, 75%).

From **5**: To a soln. of **5** (5.02 g, 17.1 mmol) in CH_2Cl_2 (170 ml) was added solid tropylium tetrafluoroborate (3.64 g, 20.5 mmol). After sonication to form a homogeneous suspension, the mixture was cooled to −78° and Et_3N (2.62 ml, 18.8 mmol) was added dropwise. After stirring for 1 h at −78°, 1M HCl was added, and the org. phase was washed with H_2O. Drying ($MgSO_4$) afforded **3** (6.83 g, 100%). Red-brown oil. IR (neat): 3022*m*, 2933*m*, 2856*m*, 2222*m*, 1656*s*, 1578*s*, 1117*s*. ^{1}H-NMR (200 MHz, $CDCl_3$): 1.92–2.07 (*m*, 1 H); 3.17 (*d*, *J* = 8.3, 2 H); 5.16 (*dd*, *J* = 9.1, 6.6, 2 H); 6.19–6.27 (*m*, 2 H); 6.62-6.75 (*m*, 2 H); 7.15 (*d*, *J* = 8.7, 2 H); 7.85 (*d*, *J* = 8.7, 2 H). ^{13}C-NMR (50 MHz, $CDCl_3$): 37.60; 38.62; 86.87; 98.87; 112.17; 122.55; 126.55; 128.65; 131.16; 133.92; 138.49; 176.84. EI-MS: 384.0 (47, M^+), 294.0 (52, $[M-C_7H_6]^+$), 255.1 (43), 166.1 (75), 152.1 (46), 139.0 (89), 127.0 (26, I^+), 91.0 (100, $[C_7H_7]^+$). HR-EI-MS: 384.0121 (M^+, $C_{18}H_{13}N_2I^+$; calc. 384.0125).

[1-(4-Iodophenyl)-2-(2,4,6-cycloheptatriene-1-ylidene)ethylidene]propanedinitrile (**4**). Compound **1** (556 mg, 1.45 mmol) was dissolved in a minimum amount of boiling hexane, and the soln. was stirred and irradiated at 366 nm at 20° for 6 h. Orange coloration and the formation of black crystals on the flask walls were observed. The crystals were collected and washed with hexane, affording **4** (491 mg). Further irradiation afforded more product (15 mg; total yield: 506 mg, 91%). A total of 40 mg (7%) of starting material **1** was recovered from the soln. Black crystalline solid. M.p. 116° (with decoloration). UV/VIS (CH_2Cl_2): 478 (33300). IR (KBr): 2957*w*, 2922*w*, 2009*s*, 1628*w*, 1512*s*, 1466*m*, 1437*m*, 1374*m*, 1344*s*, 1256*s*. ^{1}H-NMR (200 MHz, $CDCl_3$): 5.87–6.06 (*m*, 2 H); 6.29–6.48 (*m*, 3 H); 6.31 (*s*, 1 H); 6.66–6.74 (*m*, 1 H); 7.15 (*dm*, *J* = 8.7, 2 H); 7.84 (*dm*, *J* = 8.7, 2 H). EI-MS: 382.1 (100, M^+), 355.1 (36, $[M-HCN]^+$), 255.1 (94, $[M-I]^+$), 227.1 (57), 201.1 (19). Anal. calc. for $C_{18}H_{11}N_2I$ (382.20): C 56.57, H 2.90, N 7.33; found: C 56.46, H 2.91, N 7.28.

2-[1-(4-Iodophenyl)ethylidene]propanedinitrile (**5**). In a flask equipped with a *Dean-Stark* trap, a soln. of *p*-iodoacetophenone (5.00 g, 20.3 mmol) and malononitrile (2.68 g, 40.6 mmol) in PhH (200 ml) was heated to reflux for 3 d. A soln. of NH_4OAc (5 g, 64.8 mmol) in AcOH (15 ml) was added in portions during this time. After cooling to 20°, the soln. was diluted with Et_2O (200 ml) and washed with H_2O (3 × 200 ml) and sat. aq.

NaCl soln. (100 ml). Drying ($MgSO_4$), followed by CC (SiO_2-*60* (250 g); hexane/CH_2Cl_2 2:1), afforded **5** (5.29 g, 89%). Yellow crystals. M.p. 117°. IR (KBr): 2226*m*, 1580*w*, 1422*w*, 1392*m*, 1005*s*, 812*s*. ^{1}H-NMR (200 MHz, $CDCl_3$): 2.64 (*s*, 3 H); 7.30 (*d*, *J* = 9.2, 2 H); 7.89 (*d*, *J* = 9.2, 2 H). ^{13}C-NMR (75 MHz, $CDCl_3$): 23.86; 84.96; 99.34; 112.45; 112.54; 128.74; 135.18; 138.41; 174.28. EI-MS: 294.0 (100, M^+), 167.1 (12, $[M-I]^+$), 140.1 (63, $[M-I-HCN]^+$). Anal. calc. for $C_{11}H_7N_2I$ (294.09): C 44.92, H 2.40, N 9.53; found: C 44.70, H 2.20, N 9.44.

*(*E*)-1-(4-Methoxyphenyl)-3,4-bis[(triisopropylsilyl)ethynyl]-6-(trimethylsilyl)hex-3-ene-1,5-diyne* (**9**). A soln. of **6** (198 mg, 0.39 mmol), *p*-iodoanisole (182 mg, 0.78 mmol), and Bu_4NBr (4 mg, 0.01 mmol) in THF (4 ml) and a soln. of $[PdCl_2(PPh_3)_2]$ (27 mg, 0.04 mmol) and CuI (14 mg, 0.07 mmol) in THF (4 ml) and $(i\text{-}Pr)_2NH$ (4 ml) were prepared and degassed. The catalyst soln. was passed through a cannula into the soln. of **6**, and the resulting mixture was stirred for 50 min at 0° and 45 min at 20°. The mixture was diluted with hexane (30 ml), and washed with 1M HCl (30 ml) and H_2O (3 × 30 ml). Drying ($MgSO_4$) and CC (SiO_2-*60* (50 g); hexane/CH_2Cl_2 5:1) afforded **9** (76 mg, 32%) and a mixture (31 mg, 13%) of **9** and its *cis*-isomer. Yellow crystals (MeOH/AcOEt). M.p. 75°. UV/VIS (CH_2Cl_2): 264 (22400), 274 (22800), 345 (23200), 370 (*sh*, 27700), 389 (31000). IR (KBr): 2943*s*, 2864*s*, 2200*m*, 2145*m*, 1606*s*, 1514*s*, 1258*s*. ^{1}H-NMR (200 MHz, $CDCl_3$): 0.22 (*s*, 9 H); 1.12 (*s*, 21 H); 1.15 (*s*, 21 H); 3.85 (*s*, 3 H); 6.86 (*d*, *J* = 8.9, 2 H); 7.42 (*d*, *J* = 8.9, 2 H). ^{13}C-NMR (50 MHz, $CDCl_3$): −0.36; 11.22; 11.29; 18.59; 18.68; 55.29; 86.59; 98.97; 101.76; 101.89; 101.95; 103.44; 103.92; 104.21; 113.92; 114.84; 116.40; 118.21; 133.38; 160.20. EI-MS: 614.5 (100, M^+), 529.4 (11), 487.3 (15), 445.3 (26), 73.0 (14, $[Me_3Si]^+$). Anal. calc. for $C_{38}H_{58}OSi_3$ (615.14): C 74.20, H 9.50; found: C 74.01, H 9.77.

*(*E*)-1-Phenyl-3,4-bis[(triisopropylsilyl)ethynyl)-6-(trimethylsilyl)hex-3-ene-1,5-diyne* (**10**). A soln. of **6** (315 mg, 0.62 mmol), Bu_4NBr (6 mg, 0.02 mmol), and PhI (0.14 ml, 253 mg, 1.24 mmol) in THF (7 ml), and a soln. of $[PdCl_2(PPh_3)_2]$ (44 mg, 0.06 mmol) and CuI (22 mg, 0.11 mmol) in THF (7 ml) and $(i\text{-}Pr)_2NH$ (7 ml) was prepared and degassed. The catalyst soln. was passed through a cannula into the soln. of **6**, and the resulting mixture was stirred for 15 h at 20°. The mixture was diluted with hexane (20 ml) and washed with 1M HCl (2 × 20 ml) and H_2O (20 ml). The aq. layers were washed with hexane (20 ml) and the combined org. layers dried ($MgSO_4$). CC (SiO_2-*60* (50 g); hexane/CH_2Cl_2 20:1) afforded **10** (235 mg, 65%) as a yellow-brown oil, which was crystallized from MeOH. Yellow crystals. M.p. 67°. UV/VIS (CH_2Cl_2): 276 (20000), 352 (sh, 30300), 359 (31000), 377 (32709). IR (KBr): 2943*s*, 2863*s*, 2200*w*, 2133*w*, 1463*m*, 1252*m*, 1154*m*, 862*s*. ^{1}H-NMR (200 MHz, $CDCl_3$): 0.23 (*s*, 9 H); 1.12 (*s*, 21 H); 1.15 (*s*, 21 H); 7.31–7.37 (*m*, 3 H); 7.45–7.72 (*m*, 2 H). ^{13}C-NMR (50 MHz, $CDCl_3$): −0.36; 11.25; 11.32; 18.59; 18.71; 87.44; 98.52; 101.86; 102.14; 102.33; 103.32; 103.82; 104.65; 117.35; 117.92; 122.75; 128.24; 128.90; 131.82. EI-MS: 584.4 (100, M^+), 499.4 (37), 457.3 (41), 415.3 (57), 73.1 (25, $[Me_3Si]^+$). Anal. calc. for $C_{37}H_{56}Si_3 \cdot MeOH$ (617.15): C 75.95, H 10.07; found: C 75.88, H 10.11.

*2-(4-{(*E*)-6-[4-(Dimethylamino)phenyl]-3,4-bis[(triisopropylsilyl)ethynyl]hex-3-ene-1,5-diynyl}phenyl)-8a*H*-azulene-1,1-dicarbonitrile* (*trans*-**11a**). To **7** (221 mg, 0.35 mmol) in wet THF (2 ml) and MeOH (10 ml), K_2CO_3 (20 mg, 0.14 mmol) was added, and the mixture was stirred for 75 min at 20°. Dilution with Et_2O (25 ml), washing with H_2O (25 ml), and drying ($MgSO_4$), followed by evaporation *in vacuo*, gave a crude intermediate, which was dissolved together with **4** (134 mg, 0.35 mmol) and Bu_4NBr (4 mg, 0.01 mmol) in THF (8 ml). A second soln. of $[PdCl_2(PPh_3)_2]$ (25 mg, 0.04 mmol) and CuI (13 mg, 0.07 mmol) in THF (8 ml), and $(i\text{-}Pr)_2NH$ (8 ml) was prepared, and both solns. were degassed. The catalyst soln. was added *via cannula* to the soln. of **4**, and the mixture was stirred for 4.5 h at 20°. Dilution with CH_2Cl_2 (50 ml), washing with 1M HCl (2 × 50 ml) and H_2O (2 × 50 ml), drying ($MgSO_4$), and CC (SiO_2-*60* (60 g); hexane/CH_2Cl_2 1:1) afforded *trans*-**11a** (195 mg, 69%). Bright-red crystals. M.p. 219°. UV/VIS (CH_2Cl_2): 288 (40500), 402 (33300), 464 (44200). IR (KBr): 2942*m*, 2856*m*, 2200*w*, 2162*m*, 1604*s*. ^{1}H-NMR (200 MHz, $CDCl_3$): 1.15 (*s*, 21 H); 1.17 (*s*, 21 H); 3.03 (*s*, 6 H); 3.80–3.84 (*m*, 1 H); 5.85 (*dd*, *J* = 10.0, 3.7, 1 H); 6.30–6.40 (*m*, 2 H); 6.47–6.60 (*m*, 2 H); 6.65 (*d*, *J* = 8.7, 2 H); 6.95 (*s*, 1 H); 7.39 (*d*, *J* = 9.1, 2 H); 7.57 (*d*, *J* = 8.7, 2 H); 7.72 (*d*, *J* = 8.3, 2 H). ^{13}C-NMR (100 MHz, $CDCl_3$): 11.32; 11.35; 18.68; 18.72; 40.11; 45.01; 51.16; 87.07; 90.85; 96.53; 101.58; 101.68; 101.78; 103.71; 103.99; 109.26; 111.58; 112.56; 114.34; 114.99; 118.92; 119.52; 121.44; 124.77; 125.95; 127.71; 130.25; 130.88; 131.15; 132.36; 132.92; 133.26; 138.55; 139.43; 150.58. FAB-MS: 1620.5 (8, M_2H^+), 809.6 (100, M^+). X-Ray: see [17].

*2-(4-{(*Z*)-6-[4-(Dimethylamino)phenyl]-3,4-bis[(triisopropylsilyl)ethynyl]hex-3-ene-1,5-diynyl}phenyl)-8a*H*-azulene-1,1-dicarbonitrile* (*cis*-**11a**). A stirred soln. of *trans*-**11a** (38 mg, 0.047 mmol) in CH_2Cl_2 (20 ml) was irradiated at 366 nm for 3.5 h. The solvent was evaporated, and the isomers were separated by CC (SiO_2-*60* (50 g); hexane/CH_2Cl_2 1:1), affording *cis*-**11a** (15 mg, 39%). Orange crystals. M.p. 151°. UV/VIS (CH_2Cl_2): 286 (34700), 394 (56600), 464 (27800). IR (KBr): 2933*m*, 2863*m*, 2179*m*, 1604*s*, 1523*m*. ^{1}H-NMR (200 MHz, $CDCl_3$): 1.15 (*s*, 42 H); 3.03 (*s*, 6 H); 3.80–3.82 (*m*, 1 H); 5.84 (*dd*, *J* = 10.0, 3.7, 1 H); 6.29–6.40 (*m*, 2 H); 6.46–6.62 (*m*, 2 H); 6.67 (*d*, *J* = 8.7, 2 H); 6.91 (*s*, 1 H); 7.38 (*d*, *J* = 9.1, 2 H); 7.59 (*d*, *J* = 8.3, 2 H); 7.72 (*d*, *J* = 8.7, 2 H). ^{13}C-NMR (125 MHz, $CDCl_3$): 11.33; 18.72; 40.12; 45.00; 51.13; 87.37; 91.32; 96.93; 101.55; 101.85; 102.22; 103.59; 103.88; 109.13; 111.77; 112.58; 113.96; 115.00; 118.64; 119.49; 121.49; 124.82; 126.10; 127.72; 130.28; 130.89;

131.16; 132.31; 132.91; 133.12; 138.52; 139.38; 150.69. FAB-MS: 809.5 (100, M^+). HR-FAB-MS: 809.4578 (M^+, $C_{54}H_{63}N_3Si_2$; calc. 809.4560). X-Ray: see *Fig. 3*.

*2-(4-{(*E*)-6-(4-Nitrophenyl)-3,4-bis[(triisopropylsilyl)ethynyl]hex-3-ene-1,5-diynyl}phenyl)-8a*H*-azulene-1,1-dicarbonitrile* (**12**). To **8** (156 mg, 0.25 mmol) in wet THF (1.5 ml) and MeOH (7.5 ml), K_2CO_3 (16 mg, 0.11 mmol) was added, and the soln. was stirred for 1.5 h at 20°. The mixture was diluted with Et_2O, washed with H_2O, and dried ($MgSO_4$). Evaporation *in vacuo* gave a crude intermediate, which was dissolved together with **4** (94 mg, 0.24 mmol) and Bu_4NBr (3 mg, 0.007 mmol) in THF (5 ml). A soln. of $[PdCl_2(PPh_3)_2]$ (17 mg, 0.02 mmol) and CuI (9 mg, 0.05 mmol) in THF (5 ml) and (i-Pr)$_2$NH (5 ml) was prepared, and both solns. were degassed. The catalyst soln. was added *via* cannula to the soln. of **4**, and the mixture was stirred for 16 h at 20° in the dark. Dilution with CH_2Cl_2 (30 ml), washing with 1M HCl (2 × 30 ml) and H_2O (2 × 30 ml), drying ($MgSO_4$), and CC (SiO_2-*60* (50 g); hexane/CH_2Cl_2 1:1, column covered with aluminum foil) yielded **12** (104 mg, 52%). Yellow crystals (EtOH/AcOEt). M.p. 207°. UV/VIS (CH_2Cl_2): 296 (32400), 419 (54800). IR (KBr): 2944*m*, 2868*m*, 1522*m*, 1340*s*. ^{1}H-NMR (200 MHz, $CDCl_3$): 1.13 (*s*, 21 H); 1.14 (*s*, 21 H); 3.81–3.84 (*m*, 1 H); 5.85 (*dd*, *J* = 10.0, 3.7, 1 H); 6.31–6.42 (*m*, 2 H); 6.47–6.76 (*m*, 2 H); 6.97 (*s*, 1 H); 7.59 (*d*, *J* = 8.7, 2 H); 7.64 (*d*, *J* = 9.1, 2 H); 7.74 (*d*, *J* = 8.3, 2 H); 8.24 (*d*, *J* = 8.7, 2 H). ^{13}C-NMR (100 MHz, $CDCl_3$): 11.26; 18.65; 45.01; 51.12; 89.94; 92.19; 114.93; 119.51; 121.72; 123.56; 126.03; 127.76; 130.86; 131.33; 132.46; 132.55; 133.32; 138.42; 139.20; 147.38. FAB-MS: 1624.4 (28, M_2^+), 812.5 (100, M^+), 741.4 (47). Anal. calc. for $C_{52}H_{57}N_3O_2Si_2$ (812.22): C 76.90, H 7.07, N 5.17; found: C 77.18, H 7.20, N 5.28. X-Ray: see *Fig. 4*.

*2-(4-{(*E*)-6-(4-Methoxyphenyl)-3,4-bis[(triisopropylsilyl)ethynyl]hex-3-ene-1,5-diynyl}phenyl)-8a*H*-azulene-1,1-dicarbonitrile* (**13**). The entire synthesis and workup were performed under light exclusion. To **9** (73 mg, 0.12 mmol) in wet THF (1 ml) and MeOH (5 ml), K_2CO_3 (5 mg, 0.036 mmol) was added, and the soln. was stirred for 1 h at 20°. After addition of H_2O, the mixture was extracted with CH_2Cl_2, dried ($MgSO_4$), and evaporated *in vacuo* to give a crude intermediate, which was dissolved together with **4** (45 mg, 0.12 mmol) and Bu_4NBr (1 mg, 0.003 mmol) in THF (5 ml). A soln. of $[PdCl_2(PPh_3)_2]$ (8 mg, 0.01 mmol) and CuI (4 mg, 0.02 mmol) in THF (5 ml) and (i-Pr)$_2$NH (5 ml) was prepared, and both solns. were degassed. The catalyst soln. was added *via* cannula to the soln. of **4**, and the mixture was stirred for 17 h at 20°. Dilution with CH_2Cl_2 (25 ml), washing with 1M HCl (2 × 20 ml) and H_2O (2 × 20 ml), drying ($MgSO_4$), and CC (SiO_2-*60* (45 g); hexane/Et_2O 1:1) afforded **13** (52 mg, 54%). Orange crystals (EtOH). M.p. 187°. UV/VIS (CH_2Cl_2): 260 (30200), 276 (30800), 419 (56500). IR (KBr): 2945*s*, 2864*s*, 2209*w*, 1604*s*, 1509*s*, 1252*s*. ^{1}H-NMR (200 MHz, $CDCl_3$): 1.13 (*s*, 42 H); 3.81–3.84 (*m*, 1 H); 3.84 (*s*, 3 H); 5.84 (*dd*, *J* = 10.0, 3.7, 1 H); 6.32–6.39 (*m*, 2 H); 6.46–6.59 (*m*, 2 H); 6.85 (*s*, 1 H); 6.91 (*d*, *J* = 9.1, 2 H); 7.43 (*d*, *J* = 9.1, 2 H); 7.55 (*d*, *J* = 8.7, 2 H); 7.71 (*d*, *J* = 8.3, 2 H). ^{13}C-NMR (50 MHz, $CDCl_3$): 11.25; 18.62; 44.97; 51.10; 55.29; 86.84; 90.40; 97.00; 99.38; 102.21; 102.43; 103.41; 103.60; 112.52; 113.95; 114.75; 114.97; 115.98; 118.33; 119.48; 121.57; 124.46; 125.95; 127.73; 130.46; 130.87; 131.19; 132.40; 133.09; 133.44; 138.46; 139.25; 160.27. FAB-MS: 796.5 (100, M^+), 726.4 (45). Anal. calc. for $C_{53}H_{60}N_2OSi_2$ (797.24): C 79.85, H 7.59, N 3.51; found: C 79.88, H 7.51, N 3.40. X-Ray: see *Fig. 5*.

*2-(4-{(*E*)-6-Phenyl-3,4-bis[(triisopropylsilyl)ethynyl]hex-3-ene-1,5-diynyl}phenyl)-8a*H*-azulene-1,1-dicarbonitrile* (**14**). To **10** (127 mg, 0.22 mmol) in wet THF (1 ml) and MeOH (5 ml), K_2CO_3 (5 mg, 0.036 mmol) was added, and the soln. was stirred for 1.5 h at 20°. Dilution with hexane, washing with H_2O and sat. aq. NaCl soln., drying ($MgSO_4$), and evaporation *in vacuo* gave a crude intermediate, which was dissolved together with **4** (77 mg, 0.20 mmol) and Bu_4NBr (2 mg, 0.006 mmol) in THF (5 ml). A soln. of $[PdCl_2(PPh_3)_2]$ (14 mg, 0.02 mmol) and CuI (7 mg, 0.04 mmol) in THF (5 ml), and (i-Pr)$_2$NH (5 ml) was prepared, and both solns. were degassed. The catalyst soln. was added *via* cannula to the soln. of **4**, and the mixture was stirred for 17 h at 20° in the dark. Dilution with CH_2Cl_2 (25 ml), washing with 1M HCl (2 × 20 ml) and H_2O (2 × 20 ml), drying ($MgSO_4$), and CC (SiO_2-*60* (50 g); hexane/CH_2Cl_2 1:1, column covered with aluminum foil) afforded **14** (120 mg, 78%). Yellow crystals (EtOH/AcOEt). M.p. 199°. UV/VIS (CH_2Cl_2): 278 (27700), 412 (53200). IR (KBr): 2941*s*, 2864*s*, 2213*m*, 1463*m*, 1142*m*. ^{1}H-NMR (200 MHz, $CDCl_3$): 1.13 (*s*, 21 H); 1.13 (*s*, 21 H); 3.80–3.81 (*m*, 1 H); 5.84 (*dd*, *J* = 10.4, 3.7, 1 H); 6.29–6.40 (*m*, 2 H); 6.46–6.64 (*m*, 2 H); 6.94 (*s*, 1 H); 7.33–7.36 (*m*, 3 H); 7.47–7.52 (*m*, 2 H); 7.56 (*d*, *J* = 8.7, 2 H); 7.71 (*d*, *J* = 8.7, 2 H). ^{13}C-NMR (50 MHz, $CDCl_3$): 11.25; 18.62; 44.97; 51.10; 87.60; 90.24; 97.28; 98.84; 102.68; 102.81; 103.25; 103.44; 112.52; 114.97; 116.90; 118.01; 119.48; 121.63; 122.62; 124.33; 125.98; 127.73; 128.24; 128.97; 130.59; 130.87; 131.22; 131.82; 132.46; 133.16; 138.43; 139.22. FAB-MS: 766.54 (100, M^+), 696.4 (37). Anal. calc. for $C_{52}H_{58}N_2Si_2$ (767.22): C 81.42, H 7.63, N 3.65; found: C 81.37, H 7.84, N 3.56.

*2-(4-{3,4-Bis[(triisopropylsilyl)ethynyl]-6-(trimethylsilyl)hex-3-ene-1,5-diynyl}phenyl)-8a*H*-azulene-1,1-dicarbonitrile* (**15**). A soln. of **6** (96 mg, 0.19 mmol), **4** (72 mg, 0.19 mmol), and Bu_4NBr (2 mg, 0.006 mmol) in THF (5 ml), and a soln. of $[PdCl_2(PPh_3)_2]$ (13 mg, 0.02 mmol) and CuI (7 mg, 0.04 mmol) in THF (5 ml), and (i-Pr)$_2$NH (5 ml) were prepared and degassed. The catalyst soln. was added *via* cannula to the soln. of **4**, and the mixture was stirred at 20° under N_2 in the dark for 1 h. Dilution with hexane (30 ml), washing with 1M HCl

(30 ml) and H_2O (30 ml), extraction of the aq. layers with Et_2O (30 ml), drying of the combined org. phases ($MgSO_4$), and CC (SiO_2-*60* (50 g), hexane/CH_2Cl_2 2:1, column covered with aluminum foil) afforded **15** (93 mg, 64%). Yellow crystals (EtOH). M.p. 178°. UV/VIS (CH_2Cl_2): 289 (21200), 358 (28800), 404 (46700). IR (KBr): 2943*s*, 2865*s*, 2133*w*, 1464*m*, 1250*m*, 859*s*. ^{1}H-NMR (200 MHz, $CDCl_3$): 0.22 (*s*, 9 H); 1.11 (*s*, 21 H); 1.14 (*s*, 21 H); 3.80 (*m*, 1 H); 5.83 (*m*, 1 H); 6.32–6.40 (*m*, 2 H); 6.45–6.58 (*m*, 2 H); 6.93 (*s*, 1 H); 7.54 (*d*, J = 8.7, 2 H); 7.70 (*d*, J = 8.3, 2 H). ^{13}C-NMR (100 MHz, $CDCl_3$): −0.37; 11.24; 11.31; 18.63; 18.73; 45.02; 51.15; 90.05; 97.44; 101.73; 102.62; 102.95; 103.68; 105.32; 112.55; 114.97; 117.42; 117.91; 119.54; 121.59; 124.35; 125.99; 127.74; 130.60; 130.88; 131.25; 132.49; 133.14; 138.50; 139.33. FAB-MS: 762.4 (100, M^+), 736.4 (61, $[M - CN]^+$), 692.3 (85); 72.9 (46, $[Me_3Si]^+$). Anal. calc. for $C_{49}H_{62}N_2Si_3$ (763.30): C 77.10, H 8.19, N 3.67; found: C 77.04, H 7.92, N 3.70.

*2-(4-[(*E*)-6-(Thiophene-2-yl)ethynyl-3,4-bis[(triisopropylsilyl)ethynyl]hex-3-ene-1,5-diynyl]phenyl)-8a*H*-azulene-1,1-dicarbonitrile* (**16**). To **17** (120 mg, 0.20 mmol) in wet THF (2 ml) and MeOH (10 ml), K_2CO_3 (10 mg, 0.07 mmol) was added, and the mixture was stirred for 3 h at 20°. Dilution with hexane (20 ml), washing with H_2O (4 × 40 ml), drying ($MgSO_4$), and evaporation *in vacuo* gave a crude intermediate, which was dissolved together with **1** (78 mg, 0.20 mmol) in THF (5 ml). A soln. of [Pd(PPh_3)$_4$] (23 mg, 0.02 mmol) and CuI (10 mg, 0.05 mmol) in THF (5 ml) and (i-Pr)$_2$NH (5 ml) was prepared, and both solns. were degassed. The catalyst soln. was added *via* cannula to the soln. of **1**, and the mixture was stirred for 18 h at 20° in the dark. Dilution with Et_2O, washing with 1M HCl (2 × 25 ml), H_2O (25 ml), and sat. aq. NaCl soln. (25 ml), drying ($MgSO_4$), and CC (SiO_2-*60* (50 g); hexane/CH_2Cl_2 2:1, then 5:4, column covered with aluminum foil) afforded **16** (70 mg, 45%). Yellow-brown needles (EtOH/AcOEt). M.p. 222°. UV/VIS (CH_2Cl_2): 283 (28500), 420 (51300). IR (KBr): 2941*s*, 2863*s*, 2200*m*, 1655*w*, 1459*m*. ^{1}H-NMR (300 MHz, $CDCl_3$): 1.12 (*s*, 21 H); 1.14 (*s*, 21 H); 3.80–3.81 (*m*, 1 H); 5.83 (*dd*, J = 10.3, 3.7, 1 H); 6.29–6.38 (*m*, 2 H); 6.47–6.61 (*m*, 2 H); 6.93 (*s*, 1 H); 7.02 (*dd*, J = 5.0, 3.6, 1 H); 7.27 (*d*, J = 3.6, 1 H); 7.35 (*d*, J = 5.0, 1 H); 7.55 (*d*, J = 8.5, 2 H); 7.70 (*d*, J = 8.5, 2 H). ^{13}C-NMR (75 MHz, $CDCl_3$): 11.14; 18.53; 18.56; 44.90; 51.03; 90.27; 91.56; 92.19; 97.53; 102.97; 103.08; 103.13; 103.18; 112.57; 115.00; 116.51; 117.82; 119.52; 121.73; 122.65; 124.35; 126.05; 127.31; 127.81; 128.85; 130.68; 130.95; 131.31; 132.52; 133.17; 133.27; 138.51; 139.28. FAB-MS: 772.2 (100, M^+), 702.2 (23). Anal. calc. for $C_{50}H_{56}N_2Si_2S$ (773.24): C 77.67, H 7.30, N 3.62; found: C 77.66, H 7.26, N 3.61.

(Z)-2-[3,4-Bis[(triisopropylsilyl)ethynyl]-6-(trimethylsilyl)hex-3-ene-1,5-diynyl]thiophene (**17**). A soln. of **6** (251 mg, 0.49 mmol) and 2-iodothiophene (0.11 ml, 0.99 mmol) in THF (15 ml), and a soln. of [$PdCl_2$(PPh_3)$_2$] (35 mg, 0.05 mmol) and CuI (18 mg, 0.09 mmol) in THF (15 ml) and (i-Pr)$_2$NH (15 ml) were prepared and degassed. The catalyst soln. was added *via* cannula to the soln. of **6**, and the mixture was stirred for 20 min at 20°. Dilution with hexane (50 ml), washing with 1M HCl (2 × 50 ml) and sat. aq. NaCl soln. (50 ml), drying ($MgSO_4$), and CC (SiO_2-*60* (50 g); hexane/CH_2Cl_2 10:1) afforded **17** (186 mg, 64%). Yellow crystals (MeOH/AcOEt). M.p. 76°. UV/VIS (CH_2Cl_2): 283 (19800), 295 (sh, 18900), 362 (sh, 24300), 375 (25800), 394 (30400). IR (KBr): 2942*s*, 2867*s*, 2178*w*, 2133*w*, 1633*m*, 1456*m*, 1248*s*. ^{1}H-NMR (200 MHz, $CDCl_3$): 0.21 (*s*, 9 H); 1.11 (*s*, 21 H); 1.13 (*s*, 21 H); 7.00 (*dd*, J = 5.4, 3.7, 1 H); 7.24 (*dd*, J = 3.7, 1.0, 1 H); 7.33 (*dd*, J = 5.4, 1.0, 1 H). ^{13}C-NMR (50 MHz, $CDCl_3$): −0.40; 11.22; 11.29; 18.68; 91.32; 91.79; 101.76; 102.40; 102.55; 102.87; 103.63; 104.87; 116.84; 117.67; 122.68; 127.19; 128.62; 132.94. EI-MS: 590.5 (100, M^+), 505.3 (20), 463.3 (16), 421.2 (17). Anal. calc. for $C_{35}H_{54}SSi_3$ (591.13): C 71.12, H 9.21; found: C 71.23, H 9.39.

*2-(4-[3,4-Bis[(triisopropylsilyl)ethynyl]-6-triisopropylsilylhex-3-ene-1,5-diynyl]phenyl)-8a*H*-azulene-1,1-dicarbonitrile* (**18**). A soln of LDA in THF (10 ml) was prepared at 0° from (i-Pr)$_2$NH (0.12 ml, 0.82 mmol) and 1.6M BuLi (0.51 ml, 0.82 mmol) in hexane. The soln. was added *via* cannula to **20** (154 mg, 0.20 mmol) in THF (20 ml) at −78°. The resulting deep blue soln. was stirred for 15 min at this temp. before aq. workup. The crude intermediate and **1** (76 mg, 0.20 mmol) were dissolved in THF (10 ml), and a degassed mixture of [$PdCl_2$(PPh_3)$_2$] (7 mg, 0.01 mmol) and CuI (4 mg, 0.02 mmol) in THF (10 ml) and (i-Pr)$_2$NH (10 ml) was added. After stirring for 11 h under N_2 at 20° in the dark, the mixture was diluted with hexane (50 ml) and washed with 1M HCl (2 × 50 ml), H_2O (50 ml), and sat. aq. NaCl soln. (50 ml). CC (SiO_2-*60* (50 g); hexane/CH_2Cl_2 2:1, column covered with aluminum foil) afforded **18** (125 mg, 74%). Yellow crystals (EtOH). M.p. 185°. UV/VIS (CH_2Cl_2): 289 (21800), 360 (27600), 406 (46300). IR (KBr): 2943*s*, 2865*s*, 2190*w*, 2133*w*, 1464*m*, 1023*m*, 882*m*. ^{1}H-NMR (300 MHz, $CDCl_3$): 1.10 (*s*, 21 H); 1.12 (*s*, 42 H); 3.79–3.80 (*m*, 1 H); 5.82 (*dd*, J = 10.1, 3.6, 1 H); 6.29–6.38 (*m*, 2 H); 6.46–6.61 (*m*, 2 H); 6.92 (*s*, 1 H); 7.52 (*d*, J = 8.7, 2 H); 7.69 (*d*, J = 8.7, 2 H). ^{13}C-NMR (125 MHz, $CDCl_3$): 11.23; 11.26; 18.62; 18.64; 18.68; 45.00; 51.14; 90.38; 97.17; 102.35; 102.87; 102.92; 103.18; 103.80; 103.97; 112.54; 114.96; 116.85; 117.47; 119.52; 121.56; 124.41; 125.98; 127.72; 130.52; 130.87; 131.23; 132.44; 133.09; 138.49; 139.33. FAB-MS: 846.5 (100, M^+), 776.4 (54). Anal. calc. for $C_{55}H_{74}N_2Si_3$ (847.46): C 77.95, H 8.80, N 3.31; found: C 77.97, H 8.92, N 3.33.

*(*E*)-1,1-Dibromo-6-(triisopropylsilyl)-3,4-bis[(triisopropylsilyl)ethynyl]hexa-1,3-diene-5-yne* (**20**). A soln. of LDA in THF (20 ml) was prepared at 0° from $(i\text{-}Pr)_2NH$ (0.37 ml, 2.64 mmol) and 1.6M BuLi (1.67 ml, 2.64 mmol) in hexane. The soln. was slowly added *via* cannula to **19** (500 mg, 0.66 mmol) in THF (200 ml) at −78°, monitoring the reaction by TLC (SiO_2, hexane/CH_2Cl_2 3:1). The resulting green soln. was stirred for 15 min at this temp. before addition of $(i\text{-}Pr)_3SiOSO_2CF_3$ (0.65 ml, 2.44 mmol). After a couple of min, a decoloration was observed, and the temp. was raised to 0°. Sat. aq. NH_4Cl soln. (5 ml) was added, then hexane (100 ml), and the mixture was washed with H_2O (4 × 50 ml) and sat. aq. NaCl soln. (50 ml). CC (SiO_2-*60* (60 g); hexane/CH_2Cl_2 3:1) afforded **20** (438 mg, 88%). Brownish resin, which solidified after one day. IR (KBr): 2943*s*, 2865*s*, 2156*w*, 1463*m*, 1196*m*, 1037*m*, 1013*m*, 883*s*. ^{1}H-NMR (300 MHz, $CDCl_3$): 1.08–1.11 (*m*, 63 H); 7.65 (*s*, 1 H). ^{13}C-NMR (50 MHz, $CDCl_3$): 11.10; 11.20; 11.29; 18.02; 18.56; 18.69; 94.39; 100.81; 102.08; 103.15; 103.98; 104.39; 104.68; 108.52; 115.41; 130.42; 133.66. EI-MS: 752.1 (22, M^+), 625.0 (24). Anal. calc. for $C_{37}H_{64}Br_2Si_3 \cdot 0.5\ C_6H_{14}$ (839.16): C 60.35, H 8.99; found: C 60.50, H 8.81.

REFERENCES

[1] J.-M. Lehn, 'Supramolecular Chemistry, Concepts and Perspectives', VCH, Weinheim, 1995, pp. 124–138; V. Balzani, M. Gómez-López, J. F. Stoddart, *Acc. Chem. Res.* **1998**, *31*, 405.

[2] V. Balzani, A. Credi, F. M. Raymo, J. F. Stoddart, *Angew. Chem.* **2000**, *112*, 3484; *Angew. Chem., Int. Ed.* **2000**, *39*, 3348.

[3] A. P. De Silva, C. P. McCoy, *Chem. Ind. (London)* **1994**, *13*, 992.

[4] H. Kurreck, M. Huber, *Angew. Chem.* **1995**, *107*, 929; *Angew. Chem., Int. Ed.* **1995**, *34*, 849; D. Gust, *Nature* **1997**, *386*, 21, and refs. cited therein; I. Willner, S. Rubin, *Angew. Chem.* **1996**, *108*, 419; *Angew. Chem., Int. Ed.* **1996**, *35*, 367; I. Willner, *Acc. Chem. Res.* **1997**, *30*, 347.

[5] V. Balzani, F. Scandola in 'Comprehensive Supramolecular Chemistry', Vol. 10, Vol. Ed. D. N. Reinhoudt, Pergamon, Oxford, **1996**, pp. 687–746.

[6] Special Issue 'Photochromism: Memories and Switches', Guest Ed. M. Irie, *Chem. Rev.* **2000**, *100* (5), pp. 1683–1890.

[7] M. Irie, M. Mohri, *J. Org. Chem.* **1988**, *53*, 803; S. Nakamura, M. Irie, *J. Org. Chem.* **1988**, *53*, 6136; Y. Nakayama, K. Hayashi, M. Irie, *J. Org. Chem.* **1990**, *55*, 2592; M. Hanazawa, R. Sumiya, Y. Horikawa, M. Irie, *J. Chem. Soc., Chem. Commun.* **1992**, 206; K. Uchida, Y. Kido, T. Yamaguchi, M. Irie, *Bull. Chem. Soc. Jpn.* **1998**, *71*, 1101; M. Irie, O. Miyatake, K. Uchida, *J. Am. Chem. Soc.* **1992**, *114*, 8715; M. Takeshita, M. Irie, *Chem. Lett.* **1998**, 1123; S. Kobatake, M. Yamada, T. Yamada, M. Irie, *J. Am. Chem. Soc.* **1999**, *121*, 8450; K. Uchida, Y. Kawai, Y. Shimizu, V. Vill, M. Irie, *Chem. Lett.* **2000**, 654; T. Yamada, S. Kobatake, M. Irie, *Bull. Chem. Soc. Jpn.* **2000**, *73*, 2179.

[8] S. L. Gilat, S. H. Kawai, J.-M. Lehn, *Chem. Eur. J.* **1995**, *1*, 275; G. M. Tsivgoulis, J.-M. Lehn, *Angew. Chem.* **1995**, *107*, 1188; *Angew. Chem., Int. Ed.* **1995**, *34*, 1119; S. H. Kawai, S. L. Gilat, J.-M. Lehn, *J. Chem. Soc., Chem. Commun.* **1994**, 1011; S. H. Kawai, S. L. Gilat, R. Ponsinet, J.-M. Lehn, *Chem. Eur. J.* **1995**, *1*, 285; A. Fernández-Acebes, J.-M. Lehn, *Adv. Mater.* **1998**, *10*, 1519; A. Fernández-Acebes, J.-M. Lehn, *Chem. Eur. J.* **1999**, *5*, 3285; J. M. Endtner, F. Effenberger, A. Hartschuh, H. Port, *J. Am. Chem. Soc.* **2000**, *122*, 3037; C. Denekamp, B. L. Feringa, *Adv. Mater.* **1998**, *10*, 1080; F. Stellacci, C. Bertarelli, F. Toscano, M. C. Gallazzi, G. Zotti, G. Zerbi, *Adv. Mater.* **1999**, *11*, 292.

[9] B. L. Feringa, N. P. M. Huck, A. M. Schoevaars, *Adv. Mater.* **1996**, *8*, 681; N. P. M. Huck, W. F. Jager, B. De Lange, B. L. Feringa, *Science (Washington D.C.)* **1996**, *273*, 1686; W. F. Jager, J. C. Dejong, B. De Lange, N. P. M. Huck, A. Meetsma, B. L. Feringa, *Angew. Chem.* **1995**, *107*, 346; *Angew. Chem., Int. Ed.* **1995**, *34*, 348; B. L. Feringa, N. P. M. Huck, H. A. Vandoren, *J. Am. Chem. Soc.* **1995**, *117*, 9929; E. M. Geertsema, A. Meetsma, B. L. Feringa, *Angew. Chem.* **1999**, *111*, 2902; *Angew. Chem., Int. Ed.* **1999**, *38*, 2738.

[10] S. Swansburg, E. Buncel, R. P. Lemieux, *J. Am. Chem. Soc.* **2000**, *122*, 6594; M. Tanaka, K. Kamada, H. Ando, T. Kitagaki, Y. Shibutani, K. Kimura, *J. Org. Chem.* **2000**, *65*, 4342, and refs. cit. therein.

[11] Y. Yokoyama, S. Uchida, Y. Yokoyama, Y. Sugawara, Y. Kurita, *J. Am. Chem. Soc.* **1996**, *118*, 3100; Y. Yokoyama, T. Sagisaka, Y. Yamaguci, Y. Yokoyama, J. Kiji, T. Okano, A. Takemoto, S. Mio, *Chem. Lett.* **2000**, 220, and refs. cit. therein.

[12] A. M. Caamaño, M. E. Vásquez, J. Martínez-Costas, L. Castedo, J. L. Mascareñas, *Angew. Chem.* **2000**, *112*, 3234; *Angew. Chem., Int. Ed.* **2000**, *39*, 3104; Z. F. Liu, K. Hashimoto, A. Fujishima, *Nature* **1990**, *347*, 658; D.-L. Jiang, T. Aida, *Nature* **1997**, *388*, 454; M. S. Vollmer, T. D. Clark, C. Steinem, R. M. Ghadiri, *Angew. Chem.* **1999**, *111*, 1703; *Angew. Chem., Int. Ed.* **1999**, *38*, 1598.

[13] J. Daub, T. Knöchel, A. Mannschreck, *Angew. Chem.* **1984**, *96*, 980; *Angew. Chem., Int. Ed.* **1984**, *23*, 960.
[14] J. Daub, C. Fischer, S. Gierisch, J. Sixt, *Mol. Cryst. Liq. Cryst. Sci. Technol.* **1992**, *217*, 177.
[15] a) R. R. Tykwinski, F. Diederich, *Liebigs Ann./Recueil* **1997**, 649; b) F. Diederich, L. Gobbi, *Top. Curr. Chem.* **1999**, *201*, 43; c) R. R. Tykwinski, M. Schreiber, R. Pérez-Carlón, F. Diederich, *Helv. Chim. Acta* **1996**, *79*, 2249.
[16] a) R. E. Martin, J. Bartek, F. Diederich, R. R. Tykwinski, E. C. Meister, A. Hilger, H. P. Lüthi, *J. Chem. Soc., Perkin Trans. 2*, **1998**, 233; b) L. Gobbi, P. Seiler, F. Diederich, V. Gramlich, *Helv. Chim. Acta* **2000**, *83*, 1711.
[17] L. Gobbi, P. Seiler, F. Diederich, *Angew. Chem.* **1999**, *111*, 740; *Angew. Chem., Int. Ed.* **1999**, *38*, 674.
[18] a) J. Daub, S. Gierisch, U. Klement, T. Knöchel, G. Maas, U. Seitz, *Chem. Ber.* **1986**, *119*, 2631; b) A. Bäumler, J. Daub, W. Pickl, W. Rieger, *Chem. Ber.* **1985**, *118*, 1857.
[19] J. Daub, G. Hirmer, L. Jakob, G. Maas, W. Pickl, E. Pirzer, K. M. Rapp, *Chem. Ber.* **1985**, *118*, 1836.
[20] S. Gierisch, J. Daub, *Chem. Ber.* **1989**, *122*, 69.
[21] K. Sonogashira in 'Metal-catalyzed Cross-coupling Reactions', Eds. F. Diederich, P. J. Stang, Wiley-VCH, Weinheim 1998, pp. 203–269.
[22] S. Lecomte, U. Gubler, M. Jäger, C. Bosshard, G. Montemezzani, P. Günter, L. Gobbi, F. Diederich, *Appl. Phys. Lett.* **2000**, *77*, 921.
[23] R. Rossi, A. Carpita, F. Bellina, *Org. Prep. Proced. Int.* **1995**, *27*, 129.
[24] J. Anthony, A. M. Boldi, Y. Rubin, M. Hobi, V. Gramlich, C. B. Knobler, P. Seiler, F. Diederich, *Helv. Chim. Acta* **1995**, *78*, 13.
[25] M. Kaftory, M. Botoshansky, J. Daub, C. Fischer, A. Bross, *Acta Crystallogr., Sect. C* **1997**, *53*, 1665.
[26] R. R. Tykwinski, A. Hilger, F. Diederich, H. P. Lüthi, P. Seiler, V. Gramlich, J.-P. Gisselbrecht, C. Boudon, M. Gross, *Helv. Chim. Acta* **2000**, *83*, 1484.
[27] A. Hilger, J. P. Gisselbrecht, R. R. Tykwinski, C. Boudon, M. Schreiber, R. E. Martin, H. P. Lüthi, M. Gross, F. Diederich, *J. Am. Chem. Soc.* **1997**, *119*, 2069.
[28] H. Spreitzer, J. Daub, *Liebigs Ann. Chem.* **1995**, 1637.
[29] J. Achatz, C. Fischer, J. Salbeck, J. Daub, *J. Chem. Soc., Chem. Commun.* **1991**, 504.
[30] A. P. de Silva, H. Q. N. Gunaratne, T. Gunnlaugsson, A. J. M. Huxley, C. P. McCoy, J. T. Rademacher, T. E. Rice, *Chem. Rev.* **1997**, *97*, 1515; P. R. Ashton, R. Ballardini, V. Balzani, A. Credi, K. Ruprecht Dress, E. Ishow, C. J. Kleverlaan, O. Kocian, J. A. Preece, N. Spencer, J. F. Stoddart, M. Venturi, S. Wenger, *Chem. Eur. J.* **2000**, *6*, 3558.
[31] L. Gobbi, N. Elmaci, H. P. Lüthi, F. Diederich, *ChemPhysChem*, in preparation; L. Gobbi, ETH-Zürich, Dissertation No. 13535, Zürich, 2000.
[32] W. Rettig, *Top. Curr. Chem.* **1994**, *169*, 253; W. Rettig, *Angew. Chem.* **1986**, *98*, 969; *Angew. Chem., Int. Ed.* **1986**, *25*, 971; W. Rettig, R. Lapouyade in 'Topics in Fluorescence Spectroscopy', Vol. 4, Ed. J. R. Lakowicz, Plenum Press, New York, 1994, pp. 111–149.
[33] J. J. La Clair, *Angew. Chem.* **1999**, *111*, 3231; *Angew. Chem., Int. Ed.* **1999**, *38*, 3045.
[34] M. E. Huston, K. W. Haider, A. W. Czarnik, *J. Am. Chem. Soc.* **1988**, *110*, 4460; R. A. Bissell, E. Calle, A. P. de Silva, S. A. de Silva, H. Q. N. Gunaratne, J.-L. Habib-Jiwan, S. L. A. Peiris, R. A. D. D. Rupasinghe, T. K. S. D. Samarasinghe, K. R. A. S. Sandanayake, J.-P. Soumillion, *J. Chem. Soc., Perkin Trans. 2* **1992**, 1559.
[35] a) J. Daub, C. Fischer, J. Salbeck, K. Ulrich, *Adv. Mater.* **1990**, *2*, 366; b) J. Daub, S. Gierisch, J. Salbeck, *Tetrahedron Lett.* **1990**, *31*, 3113.
[36] M. R. Winkle, J. M. Lansinger, R. C. Ronald, *J. Chem. Soc., Chem. Commun.* **1980**, 87.
[37] G. M. Sheldrick, *Acta Crystallogr., Sect. A* **1990**, *46*, 467.
[38] G. M. Sheldrick, SHELXL-93, 'Program for the refinement of crystal structures', University of Göttingen, 1993.

Received December 19, 2000